UNIVERSITY OF OKLAHOMA

GRADUATE COLLEGE

THE "U-TUBE": AN IMPROVED ASPIRATED TEMPERATURE SYSTEM FOR MOBILE METEOROLOGICAL OBSERVATIONS, ESPECIALLY IN SEVERE WEATHER

A THESIS

SUBMITTED TO THE GRADUATE FACULTY

in partial fulfillment of the requirements for the

Degree of

MASTER OF SCIENCE IN METEOROLOGY

BY

SEAN MICHAEL WAUGH
Norman, Oklahoma
2012

Acknowledgements

I would sincerely like to thank Mr. Sherman Fredrickson for his help throughout my entire career thus far. The work presented in this thesis was done as a collaborative project and without his guidance and mentoring it would not have been possible. He presented ideas and solutions throughout the design and testing process that helped craft the research presented herein to its current potential. I cannot take sole credit for this work as he was as intricately involved as I was in the process.

Furthermore, he has become a great mentor and friend, providing his insights on issues throughout my work and helping me to become a better researcher. His unique perspective on teaching has provided an excellent learning environment that has helped me to think more critically about almost everything in life.

I would also like to thank Drs. Biggerstaff, Fiedler, Klein, and Straka for their help with this process. My decision to get a Master's degree was a rather late decision and they have been extremely accommodating. Their patience with me during the last few months is much appreciated. Dr. Dave Rust for allowing me to take time away from my other research, NSSL and the entire staff of the VORTEX 2 project for allowing me to use project vehicles for the testing of the various instrument housings. The data sampled during the study would have been impossible to sample otherwise. This work was partially funded by the grant NSF AGS-1036237.

Table of Contents

List of Figures

List of Equations

Abstract

The ability to obtain quality air temperature measurements in and around thunderstorms is often problematic, and even more challenging from a moving platform such as a ground-based vehicle. Since the original Verification of the Origin of Rotation in Tornadoes Experiment (VORTEX) project in 1994-1995, mobile weather platforms known as Mobile Mesonets (MMs) from the National Severe Storms Laboratory (NSSL) and the Center for Analysis and Prediction of Storms (CAPS) have used an aspirated temperature shield design called a "J-Tube" that address some, but not all of the issues commonly encountered. Due to these concerns, for VORTEX 2: 2009 an R.M. Young model 43408 temperature shield was added to complement the J-tube. However, it too was found to have certain shortcomings in severe weather environments. Between the end of VORTEX 2: 2009 and the start of VORTEX 2: 2010, a third new and new shield was designed, tested and installed called the "U-Tube."

The results of efforts to better characterize the J-Tube, the RM Young shield, and the design and performance characteristics of the U-Tube, in and around thunderstorms, are reported. Additionally the entire 2010 season of the VORTEX 2 project was used for an intercomparison of these shield designs. Results indicate that compared to the J-tube and the RM Young shield, the U-tube improves the response time, and reduces errors due to solar radiation, rain, varying wind directions, and speed.

Chapter 1: Introduction

Surface temperature measurements from a typical stationary weather site can be problematic for severe weather studies. The site must wait for the weather to come to it, and the sensors in use must be able to perform well in both severe and benign conditions. A mobile platform offers the advantage of being able to move to where the weather is, but brings with it the added complexity of obtaining accurate measurements while under constantly changing conditions. Additionally, on a mobile platform weather conditions are typically encountered at a much higher speed than on a stationary site.

For the original Verification of the Origin of Rotation in Tornadoes Experiment (VORTEX) project in 1994-1995, a fleet of fifteen mobile weather platforms, known as Mobile Mesonets (MMs), were designed collaboratively by the National Severe Storms Laboratory (NSSL), the Center for Analysis and Prediction of Storms (CAPS), and to some degree the University of Oklahoma, School of Meteorology (SOM) (NSF grant ATM91-20009 supported this effort). Details of these MMs, including the sensors, the systems housing them, the design, and implementation of the vehicle have been described in detail by Straka et al (1996).

These vehicles were designed specifically for the VORTEX project and consequently the specific purpose of cloudy, convective weather research (as opposed to sunny, low wind, benign conditions). In doing so, several considerations for the

instruments chosen were downplayed due to their relative unimportance during these specific environments. A good example of one such consideration would be solar radiation errors. While typically an important consideration for a temperature shield, high values of incoming solar radiation are not commonly encountered on a project studying convection. As such, the temperature shields at the time did not necessarily need to be able to perform adequately during such conditions.

However, since their inception, the MMs vehicles have been used in a variety of field programs spanning a wide range of conditions (VORTEX, IHOP, STEPS, Hurricane Ike 2008, VORTEX 2, and Hurricane Irene 2011 to name a few) [Buban et al. 2002, Markowski 2002a, Markowski 2002b, Markowski et al. 2002; Lang et al. 2004, Pietrycha and Rasmussen 2004, Shabbott and Markowski 2006, Grzych et al. 2007, Stonitsch and Markowski 2007, Hirth et al. 2008]. As demonstrated by their extensive usage, the ability of the MM to collect *in situ* observations while on the move is a much desired feature. Unfortunately, some of these applications are outside of the conditions that the MMs were originally designed to operate in during data collection.

Additionally, several other groups have realized the usefulness of the MM and have since copied the design, in whole or in part, for their own use (examples include Karstens et al. 2010, Taylor et al. 2011, Skinner et al, 2011, Lee et al. 2011). With this design spreading throughout the meteorological community, it is imperative that the MM be examined for limits on what types of conditions it should be used in. If

situations do exist where the current Mobile Mesonet is unable to perform adequately, changes should be made to the system to make it more adaptive to a wider range of circumstances.

Chapter 2: Background

Obtaining the highest quality data possible over a variety of circumstances is not as simple as choosing the fastest response sensor. There are many considerations, that mobile platforms and stationary sites share to varying degrees, which must be made to ensure quality data that are as free as possible from avoidable errors. These considerations not only influence the sensors chosen, but the design of the shields in which the instruments are placed, the location in which the shields are mounted on the platform, and ultimately, the conditions in which the platforms are used. A generalized example of some of these considerations is examined shortly, including solar radiation, aspiration rate, changes in the ambient wind speed and/or direction, rain (wet-bulb errors), and the overall response time of a system.

A. General considerations

i. Temperature Errors caused by Solar Radiation

Solar radiation errors are of major concern to a stationary network (Brasefield 1948, Fuchs and Tanner 1965, Hubbard et al 2004). These errors are

more prevalent during low wind conditions as most stationary networks use some variation of a naturally aspirated multiplate radiation shield (Richardson 1995, Nakamura and Mahrt 2005). Because of power restrictions, many stationary networks cannot avoid this issue and thus, have to accept that these errors may be present (Brock et al. 1995). There are however three main ways to reduce the effect of solar radiation on temperature measurements. The shield must: 1) reduce the radiation that is able to directly or indirectly (by reflection) reach the sensor, 2) maximize the airflow around the sensor, and 3) reduce or properly remove the radiation absorbed by the shield itself (Richardson et al. 1999). Toward this end many temperature shields have a double walled, downward pointing intake, which reduces the amount of solar radiation that is incident on the sensor. Furthermore, the shield is typically constructed from a material that is highly reflective and has a low capacity to absorb heat so that re-radiation errors can be reduced.

While following the previously mentioned guidelines may work well for a stationary site located over grassy terrain, vehicles present an additional concern. Most vehicles are painted with a highly reflective glossy paint. This results in a strong reflectance of incoming solar radiation, increasing the total amount of incoming solar radiation on a temperature shield. Given the placement of a temperature shield on a vehicle, this could result in solar

radiation angles that allow radiation to directly reach a sensor. Furthermore, the vehicle itself will absorb and re-radiate energy, further complicating the placement of a temperature shield. In short, the temperature shield must be able to reflect or redistribute heat caused by high solar radiation from a large range of incoming angles.

ii. Aspiration Rate

Previous studies have documented that naturally aspirated radiation shields are incapable of providing sufficient air exchange between the shield and the ambient air outside the shield when wind speeds are less than 5 ms^{-1} (Richardson et al. 1999, Lin et al. 2001b). As the natural wind speed drops, the exchange rate in the radiation shield also drops to the point where the temperature sensor begins to become decoupled from the ambient environment. This leads to an increased response time of the measurements and introduces exposure errors that can exceed those errors normally associated with the sensor itself.

For stationary sites, this is particularly problematic due to power limitations as mentioned previously. While solar panels and back up batteries can be used, many other pieces of equipment on these sites can consume a considerable amount of power necessitating a balancing act. On special stationary sites and vehicles, such as the MM, this is not the case and small DC fans can be used to supplement the aspiration rate of a temperature shield. This

provides sufficient air exchange throughout the system during conditions where there is little or no ambient wind.

It is vital that a temperature shield maintain an adequate air exchange rate with the ambient environment. A high exchange rate allows the system to respond quickly to a change in temperature. This is particularly important on a mobile platform as temperature changes can be encountered at a much higher rate of speed.

iii. Temperature Errors caused by changes in ambient wind speed or direction

Stationary sites typically encounter relatively benign conditions over most of their data collection. As such, sharp changes in the ambient wind speed and/or direction do not occur frequently, and only periodically do stationary networks encounter winds above the National Weather Service established severe threshold (58 mph). More importantly, when these events do occur, they typically last for only brief periods of time when compared to the typical environments encountered. Stationary networks, therefore, do not require their temperature shields to explicitly be able to handle high wind environments constantly. Thus in the past, most studies examining the airflow characteristics of a temperature shield in changing wind conditions were focused on low speed cases for use in estimating solar radiation errors (Lin et al 2001a).

High wind conditions are an almost constant issue on a mobile platform however. The relative wind speed and direction over a vehicle is a combination of the vehicle motion and the ambient winds. This relative wind can easily reach speeds over 60 mph (26.8 ms^{-1}) and is often in the range of 80-120 mph (35.8-53.6 ms^{-1}), with extreme cases potentially reaching as high as 120-140 mph (53.6-62.6 ms^{-1}). Since the vehicle can be constantly turning and changing its direction within the ambient flow, the relative wind direction over the vehicle can also be constantly changing.

Any temperature shield placed on a mobile platform such as the MMs would need to be able to handle constant fluctuations in the wind. Ideally, the aspiration rate through a temperature shield would increase with the increasing relative wind speed and would be unaffected by changes in the relative wind direction to ensure optimal air exchange.

iv. Temperature Errors caused by Rain

Inevitably, while making temperature measurements on either a stationary site or a mobile platform, rain is encountered. This can be problematic depending on the temperature shield chosen as large errors in temperature can occur due to wet-bulbing (Lenschow and Pennell 1974, Heymsfield et al. 1979, Lawson and Cooper 1990, Eastin et al. 2002). This error occurs as rain, which wets a temperature sensor or the shield containing it evaporates in an

unsaturated environment, leading to cooling of the sensor below the actual air temperature. Snow, drizzle, mist, and spray off the roadway or other vehicles are also potential sources of this error. Several temperature shields, such as a naturally aspirated multiplate radiation shield, are particularly susceptible to this problem and have been avoided in previous mobile observing systems (Straka et al. 1996).

To minimize these errors, temperature shields often place the sensor far enough inside a shield to reduce the likelihood of rain wetting the sensor. For a stationary network, this is accomplished relatively easily for most conditions, but can become problematic in high wind conditions. In this situation the high wind can drive rain further inside a shield than normal. A mobile platform will have this issue at any time when encountering rain while moving due to the constant presence of high winds. The smaller or more light-weight the particles become, the harder it is to separate the liquid (or frozen) water from the air stream.

As an added difficulty, mobile platforms can enter and exit regions of rain quickly, further compounding wet-bulb errors if water remains on the sensors or shield by driving into an unsaturated environment. With these concerns, a temperature shield should be able to not only protect a sensor from

being wetted during rain, but also quickly shed any water that is present once a region of rain is exited.

v. Temperature Errors caused by the Overall Response Time

The time constant of a system is what ultimately determines how fast that system will respond to a change in temperature. No matter how accurate a sensor is, a slow time constant will result in changes in temperature being smoothed out and misrepresented from the actual truth that occurred. A "gradient dampener" is a good term for this type of behavior, as coined by a personal conversation with Sherman Fredrickson. Large differences between the measured temperature and the actual temperature can occur simply due to the time constant of a given temperature sensor, depending on how fast a temperature change occurs. This error becomes larger the faster a change in temperature occurs.

This time constant is not just given by the temperature sensor used, but is also affected greatly by the radiation shield used. Upstream thermal mass can modify the measured air prior to reaching the sensor (Fuchs and Tanner 1965) and a low aspiration rate throughout the system can increase the response time by slowing down the mixing with the ambient environment (Lin et al 2001a).

Since mobile platforms experience changes in temperature at potentially rapid rates, it is critically important that the response time of a temperature

system be as fast as possible to accurately reflect the temporal and spatial changes in the ambient environment.

B. Mobile Mesonet Specific Consideration: Hail

While the previously mentioned considerations are all very important, there is an additional consideration that comes into play when considering a mobile platform such as a MM. When used by NSSL, these systems are often times repeatedly exposed to severe weather conditions, specifically hail. While sporadically encountered on a stationary network, a MM can encounter large hail (baseballs or larger) frequently, depending on its use. Constantly having to replace instrumentation due to damage adds an increased cost to any project and degrades the usefulness of that system until the damage is repaired. As such, the instrumentation used on a MM must be rugged enough to withstand the constant punishment of these severe conditions without compromising performance and prevent damage to expensive instruments.

Chapter 3: Mobile Mesonet Temperature Shields

With the above considerations as guidelines, there are several possibilities of temperature shields that could be used for mobile temperature applications. Several commercially available shields could potentially be used,

as well as a few hand-made designs. In the past, NSSL has used two temperature shields on the MMs: an in-house design known as the J-tube, and an RM Young model 43408.

A. Historical Approach: The J-tube

i. Design

When the original VORTEX era MMs were built, an R. M. Young model 41002 naturally aspirated multiplate radiation shield was used to house the temperature sensors. This was done in an attempt to protect the sensors from direct solar radiation and rain (Straka et al. 1996). It was found through testing and observation, however, that that the sensors and shield were easily wetted in rainy, windy conditions and stayed wet after the rain had ended. This behavior led to large wet bulb errors in the measured temperature, which were not acceptable for MM applications. In an

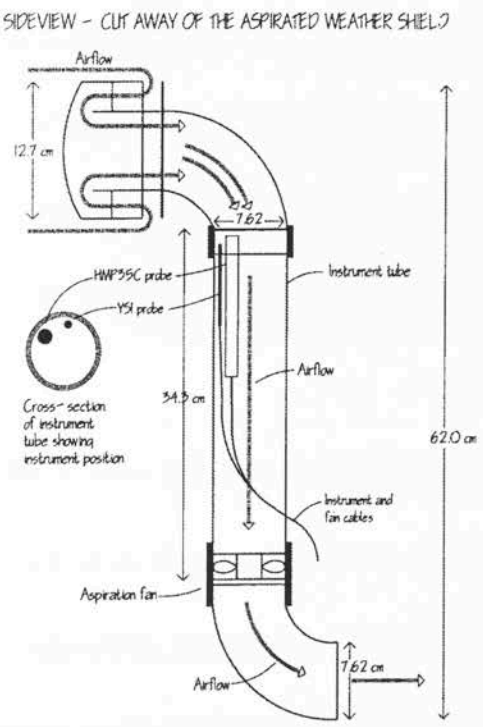

Figure 1: J-tube cross section indicating airflow patterns and instrument locations. The structure is made from schedule 40 PVC and includes a DC fan in the exhaust for aspiration (Straka et al. 1996).

attempt to combat this issue, a new radiation shield known as the J-tube was created for the VORTEX project (Straka et al., 1996) (Fig. 1).

The J-tube is constructed from schedule 40 white polyvinyl chloride (PVC) that is approximately ¼" thick and 3" wide, which provides adequate strength against severe weather impacts. A small DC fan is located near the exhaust portion of the J-tube to help aspirate the unit in the absence of ambient winds; however, the aspiration rate was primarily intended to be forced by the local wind and differential pressures (Bernoulli Effect) that are directly present over the roof of the vehicle. This fan has been changed periodically throughout the years since its inception and is currently a 0.55 amp, 30 ft^3/min [0.014 m^3/s] fan. The design of the J-tube was modeled after a "reverse flow" temperature shield for aircraft created by Rodi et al., 1972 (per personal conversation with Sherman Fredrickson).

In both the Rodi shield and the J-tube, airflow entering the intake portion of the shield is required to make several sharp turns that mechanically separate water droplets from the airflow. From this separation, liquid water is shed from the airflow before reaching the sensor and thus, wet bulb errors are reduced. The unit is mounted on vehicles with the intake facing forward with respect to the front of the vehicle in an attempt to maximize the airflow over the intake, which is required for water separation. The design of the shield allows several

temperature sensors to be placed inside, so that both temperature and relative humidity can be measured in the same unit.

ii. Potential Sources of Error

As was mentioned earlier, the J-tube was designed with the express purpose of being used on a mobile platform that is constantly in motion and during cloudy, convective weather only. The creators had no intention that the unit be used outside those specific conditions. As such, there are several conditions under which the behavior of the J-tube is not well documented and could lead to errors in the measured temperature.

a. Changes in Wind Speed/Direction

The J-tube was not designed to be used in prolonged situations with light winds or winds from any other direction other than straight on with the front of the vehicle. It was assumed that if constantly in motion, the relative wind over the vehicle created by the motion of the vehicle itself, would keep the wind oriented at the intake of the J-tube. However, the orientation of the vehicle with respect to the ambient wind cannot be guaranteed. There exists the potential that if the vehicle is stationary or moving slowly with respect to the ambient wind, that the direction of the relative wind over the vehicle may not be from the front. The geometry of the shield results in a directional sensitivity and the behavior of

the aspiration rate with respect to changes in the relative wind speed or direction is unknown.

b. Solar Radiation

With the applications intended by the creators, considerations of solar radiation errors were not needed. The shield design does protect the sensors from direct solar radiation, but re-radiation of energy absorbed by the shield is of concern. Though the PVC is painted with a reflective white paint, it tends to absorb and hold energy, both from its surroundings and from direct solar radiation, and transfer that energy to the sensed air passing by the surface leading to errors in the measured temperature. It was estimated by Dr. Straka during initial testing, that the J-tube likely experiences errors from 0-3°C during strong solar heating (Straka et al. 1996), but a more definitive description of this behavior is unknown.

c. Overall Response Time

Finally, the aspiration rate and overall response time of the J-tube system is generally undocumented. While the intake head of the J-tube is useful for separating water from the airstream during rain and shielding the sensors from direct solar radiation, it also provides upstream thermal mass that could act to modify the air mass prior to being sensed and effectively increase the response

time. The flow rate through the system could help to mitigate this problem, but is undocumented.

B. A Response to Concerns: The RM Young Model 43408

With the 2009 season of VORTEX 2 quickly approaching, it was determined that due to the uncertainties, the J-tube alone would not be suitable for all possible MM applications. To address this issue, a second temperature shield was added to the MM system in an attempt to cover situations with possible errors. The shield chosen by NSSL was an R.M. Young Model 43408 Gill Aspirated Radiation Shield (Fig. 2) and was used in conjunction with the J-tube during the first phase of the project.

Figure 2: RM Young Model 43408 aspirated temperature shield. Unit is mounted horizontal to the surface and has an extendable intake. The intake houses a single sensor and flow rates through the system vary between 3 ms^{-1} and 7 ms^{-1} depending on the sensor used.

i. The RM Young 43408

This system was chosen specifically for performance under high solar radiation and the proximity of the temperature sensor to the intake. The RM

Young is typically used as a reference in high solar radiation situations (Richardson et al. 1999, Anderson et al. 1998, Hubbard et al. 2005, Brandsma and Vander Meulen 2008) and experiences less than +/- 0.02 °C error under 1100 W/m^2 per the manufacturer specifications. Flow rates through the system vary between 3 and 7 ms^{-1} depending on the sensor used in the housing. Though not specifically documented, the proximity of the sensor to the intake was thought to provide a fast response time for the system, depending on the sensor chosen.

ii. Potential Sources of Error

With its potentially fast response time and low solar radiation errors, the RM Young is well suited for temperature measurements on a stationary site, but was not intended to be used in the conditions surrounding a mobile platform. Like the J-tube, the RM Young has several areas where the potential for errors exists due to undocumented responses of the unit.

a. Changes in Wind Speed/Direction

The RM Young has no documentation regarding how the aspiration rate of the unit is affected during changes in the relative wind direction or speed. As mentioned before, both of these conditions are common on the MM and should

be explored. However, due to the symmetric nature of the intake it was not expected to be of significant concern.

b. Rain.

With the proximity of the temperature sensor to the opening of the intake and the high aspiration rates possible depending on sensor size, it is conceivable that the RM Young could experience wet-bulb errors during periods of rain. Brandsma and Van der Meulen, 2008 noticed this behavior during one of their tests while using this radiation shield, though they did not examine it further. As such, additional documentation of this error is needed.

Chapter 4: J-tube and RM Young Characterization

Prior to the beginning of the 2009 season of VORTEX 2, a short series of tests were completed to characterize the two temperature shields that would be in use and determine if a combination of the J-tube and the RM Young would be adequate. Three specific areas were tested: aspiration response to changes in the relative wind direction, aspiration response to changes in the relative wind speed, and the overall response time of the system.

A. Effects of Relative Wind Direction on Aspiration Rate

i. Experimental Setup

In order to test the response of the aspiration rate inside both the J-tube and the RM Young during changes in the relative wind direction, a MM with both systems mounted on the rack was used. This was the same setup that was deployed for the 2009 season of VORTEX 2 and, with the exception of the RM Young, is the same basic design as the original MM (Straka et al. 1996). The MM was taken out to the Lloyd Noble Center parking lot (located at 2900 S. Jenkins, Norman, OK 73019) on a day during which the winds were relatively constant at approximately 8 mph (3.6 ms^{-1}). While there were some natural fluctuations in the wind speed and direction, the wind was primarily out of the north. The parking lot was chosen owing to its wide open area so that flow distortions from objects upstream would be minimized. While turbulence was not strictly measured during the test, any distortions would be evident in the data collected from the MM rack as sudden changes in the speed or direction.

In order to measure the aspiration rate inside each of the temperature shields, a Thermo Systems Inc. (TSI) Model 8455-06 Hot Wire Anemometer was used. The small probe on the end of the anemometer allowed the flow rate to be measured inside each of the systems without significantly obstructing the air flow pattern. In both shields, the hot wire anemometer was mounted such

that the air flow measurements were being taken at the location of the temperature sensors.

In addition to the hot wire anemometer, a DC generator fan was placed into the J-tube. This was done due to concerns with its potential directional sensitivity. It was conceivable that the aspiration rate could potentially slow to zero, and eventually reverse direction. The DC generator produces a voltage signal proportional to the speed and direction at which the fan is spinning. The unit was mounted such that when operating correctly, the aspiration rate would produce a positive voltage. If the aspiration rate were to reverse directions, the polarity of the voltage signal from the DC generator would switch to negative, indicating the reversal of flow. Because the generator would provide some resistance to the flow, it is conceivable that the flow rate of the J-tube could be affected by this instrument. This effect was tested, and found to be minimal through comparison with and without the generator. The signal from the DC generator and both of the hot wire anemometers were recorded onto a Campbell Scientific CR-10X datalogger, along with the relative wind speed and direction from the MM.

Initially, the stationary vehicle was pointed nose first into the wind to start data collection with the theoretical best possible operating conditions for the J-tube. After five minutes, the vehicle was turned 45° clockwise and then left

for an additional five minutes. This process was repeated over the course of an entire 360° rotation so that the relative wind direction was manually varied across the vehicle. By doing these rotations, the relative wind direction surrounding each of the temperature shields could be manually controlled and changed in order to document the aspiration rates response to those changes. The vehicle was left in each position for five minutes in an effort to produce an average to reduce the effects of any variations in the ambient wind.

ii. Results

Following the data collection period, the relative wind direction from the MM along with the aspiration rates in both the J-tube and the RM Young were plotted and the data are shown in Fig. 3. The figure shows that while the flow rate in the RM Young is relatively unaffected by changes in the relative wind direction, the opposite is true for the J-tube.

The maximum flow rate for the J-tube (approximately 2 ms^{-1}) is obtained when the relative wind direction is from the front of the vehicle (ie. directed at the intake of the J-tube). This is the ideal, and intended, operating orientation for the J-tube. From this point, the aspiration rate begins to decrease as the relative wind direction moves clockwise toward the rear of the vehicle. At several points, the aspiration rate inside the J-tube slows to zero, and eventually completely reverses directions as indicated by the red points in the figure.

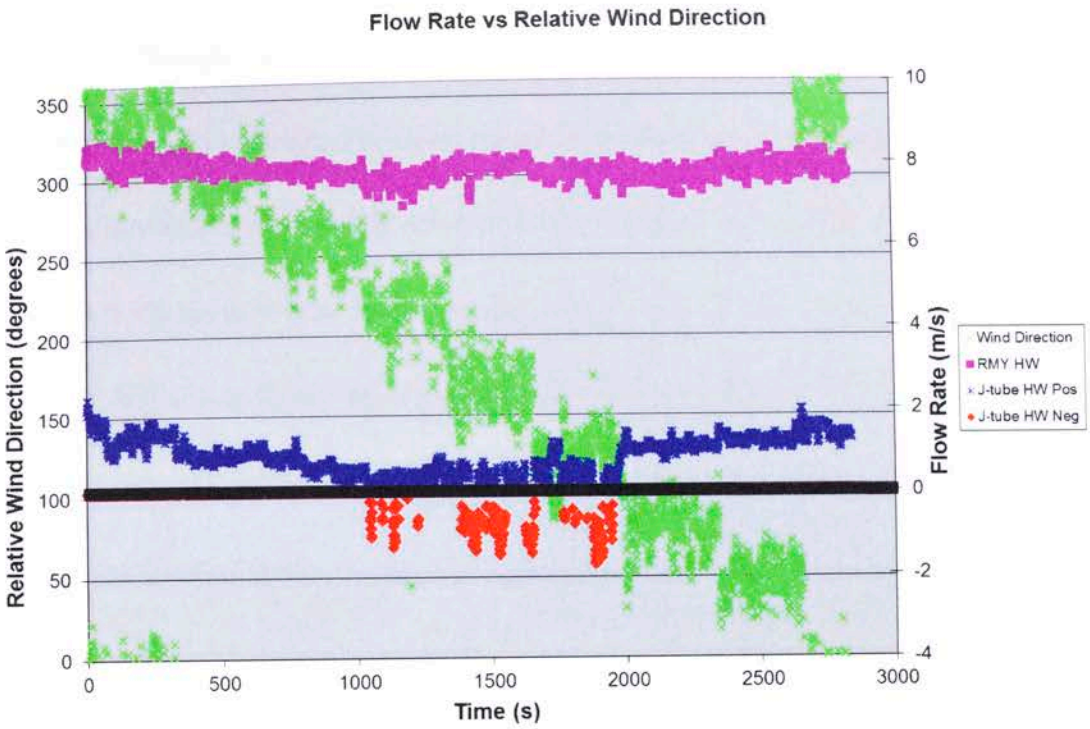

Figure 3: J-tube/RM Young aspiration rates as a function of relative wind direction. Green 'x' markers indicate the relative wind direction on the left axis as it was varied in steps across the vehicle. The purple squares show the flow rate of the RM Young (RMY HW) on the right axis and that it is relatively unaffected by changes in the wind direction. The blue 'x' points indicate the J-tube's flow rate on the right axis and its sensitivity to the relative wind direction. Red diamond points indicate negative flow rates in J-tube. The bold, solid black line highlights the zero line for aspiration.

The reduction in aspiration rate occurs as the relative wind over the vehicle begins to compete with the fan located in the exhaust of the J-tube. At some point the relative wind overpowers the fan, and the aspiration rate eventually reverses direction. This can cause problems when making temperature measurements as the temperature shield is no longer operating as intended. Heat from the fan, reradiation off the vehicle roof, and water spray off the roof all are now possible which could introduce errors into the system. Aditionally, as the flow rate slows to near zero, the unit is becoming decoupled from the ambient envionment which can also lead to temperature errors.

Though the directionality test was completed while the MM was stationary, this scenario is quite possible while moving depending on the speed and direction of the vehicle relative to the ambient winds. An example would be driving along in a gust front scenario where the vehicle speed is 40 mph (17.9 ms^{-1}), but the ambient wind speed is 60 mph (26.8 ms^{-1}) in the same direction. The result of this would be a tail wind over the vehicle which would compete with the fan and result in reverse aspiration. In this example scenario, the flow is higher than was tested so the flow rate could be expected to be more of a negative than shown in Figure 3.

B. Effects of Relative Wind Speed on Aspiration Rate

i. Experimental Setup

In order to test each of the shields aspiration rate response to changes in the relative wind speed, the same MM as used in Section IV.A. was taken out to an area on 60th Ave NW, north of Robinson St. in Norman OK, commonly referred to as the "Ten Mile Flats," which is just west of town. At this location, the road is oriented north-south and is in a semi-rural area. There are no ditches next to the road, little traffic, and the road is located in flat and open terrain with a few homes set off the road by a few 10s of meters. This location was chosen as it allowed the MM to be driven with minimal considerations to influence by other vehicles or turbulence from nearby objects, and is relatively free from any

drainage flow due to terrain. To further simplify the experiment, this test was done at night (2 am local time) during calm conditions (<10 mph [4.5 ms^{-1}] ambient winds). Being late at night, the local traffic and any local turbulence due to solar radiation was also reduced.

With this setup an artificial wind could be created over the vehicle by simply driving at a desired speed. Since there was no ambient wind present, the relative wind was straight on from the nose of the vehicle and was controlled by the speed of the vehicle. In this manner, the vehicle was driven at various desired speeds (within limits for legal and safety reasons) and the aspiration rate through the shields measured. This test was done with the shields mounted in their normal operating orientations. It was assumed that any influence the relative wind speed had on the aspiration rate would be symmetric about the shield and would simply magnify the directional sensitivity discovered previously.

During the test, the MM was driven in a straight line down the road at speeds of 10 mph, 20 mph, 30 mph, 40 mph, 50 mph, 60 mph, and 70 mph (4.5, 8.9, 13.4, 17.9, 22.4, 26.8, and 31.3 ms^{-1} respectfully) in a step-wise fashion, for approximately 30 seconds at each speed. The 30 second requirement was established to give each system time to stabilize so that a better sense of the normal flow rate at a given relative wind speed could be gained. The length of

time was determined in previous test runs by examining if preliminary data for any lag in the response of each unit. There was none, so a 30 second time frame was more than adequate.

As before, the internal flow rates of each temperature shield were measured using a TSI Hot Wire Anemometer. The setup for the mounting of the hot wire was the same as was used previously. This, along with the relative wind speed and direction as measured by the MM, were recorded on a CR-10X datalogger.

ii. Results

After completing several trail runs of the experiment, the data was examined to determine a relationship between the relative wind speed over the vehicle and the aspiration rate inside each of the temperature shields. This data are summarized in Fig. 4. The graph shows that the RM Young has a negative sensitivity in aspiration rate (decrease of approximately 2 ms^{-1}) due to changes in the wind speed. Conversely, the J-tube respondes positively to increasing speeds (increases from 2 ms^{-1} to nearly 11 ms^{-1}).

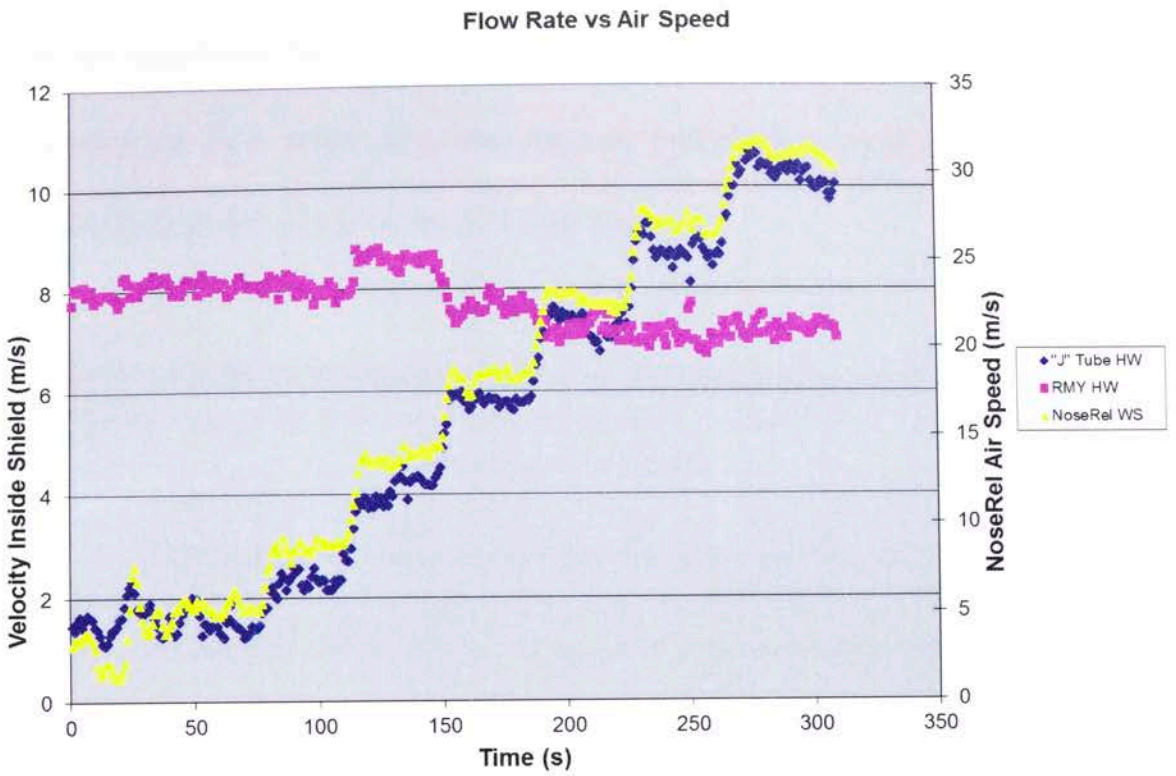

Figure 4: J-tube/RM Young aspiration response as a function of relative wind speed over the vehicle. The yellow triangles indicate the relative wind speed over the vehicle on the right axis. The purple squares indicate the RM Young aspiration rate on the left axis and its tendency to decrease with increasing relative wind speed. The blue diamonds indicate the J-tube's aspiration rate (right axis) and its tendency to increase with increasing relative wind speed.

The J-tubes' aspiration is achieved from two sources: the DC fan and a Bernoulli process that is occuring over the roof of the vehicle. As the car accelerates, flow is forced upwards over the roof of the vehicle and is accelerated faster than the ambient speed due to a reduction in the cross sectional area in the flow field. The exhaust portion of the J-tube is located within this accelerated air stream (or slip stream), but the intake is not (See Straka et al. 1996 for figure of smoke slip stream over a vehicle). Neglecting variations in density (imcompressible fluid) and assuming that the height change

is not significant, Bournoulli's prinicple (Eq. 1) can be used to show that the accelerated flow leads to a low pressure perturbation, with respect to the unaccelerated flow over the intake of the J-tube.

$$\frac{v^2}{2} + gz + \frac{P}{\rho} = C$$

Equation 1: Incompressible flow equation from Bernoulli's Principle. V is the velocity of the fluid, g is acceleration due to gravity (9.81 m/s2), z is the elevation above a reference place, P is pressure, ρ is the density, and C is a constant.

The result is a difference in static pressure between the intake and the exhaust that causes a flow field to form in the direction of the pressure gradient (PG). Thus, as the car accelerates, the speed of the air stream over the car likewise increases. This increased pressure gradient across the J-tube then in turn produces an increased aspiration rate.

With this behavior, as an observer drives the MM faster, or drives into increasing ambient head winds, the flow rate through the J-tube is constantly increasing. By increasing the flow rate, air is cycled through the system at a much faster rate (up to 8 ms^{-1} faster depending on vehicle speed), reducing the amount of time that sensed air mass is in contact with any upstream thermal mass. This would tend to reduce any air mass modification prior to sensing and would increase the response time of the system by quickly changing the temperature. This behavior is useful as the J-tube will respond faster to fluctuations in tempearture (within the limitations of the sensor) as the MM is moved through those changes faster.

C. System Response Time

i. Experimental Setup

The simplest way to determine the response time of a temperature system is to put that system through a step change (instantaneous) in temperature. Unfortunately, putting an entire MM through a sharp step change in temperature is complicated, so a smaller cart mounted version of the MM rack was created (Appendix A, Fig 1). The smaller, modified rack was outfitted with an RM Young Wind Monitor, a J-tube, and a RM Young 43408. This setup allowed the instruments to more easily be simultaneously put through a step change in temperature, while the temperature data inside each of the shields was recorded.

To achieve the largest step change possible, the NSSL vehicle bay was utilized during the winter months. The vehicle bay is heated while the outside is cold, producing a large step change in temperature by moving the cart mounted rack between the vehicle bay and outside. The actual magnitude of the step change is not particularly important, but a larger step change will make the interpretation easier.

To simplify the experiment, the test was completed late at night (approximately 2 am local time) during calm wind conditions. This was done to ensure that solar radiation errors could be neglected, turbulence was minimal,

and that the aspiration rate through the shields was due only to their respective fans. This test respresents the response of each system under an exact set of conditions and cannot be used as a correction factor.

To determine the time constant of each shield, the method as outlined by Brock and Richardson (2001) was used. Equation 2 shows a generalized step-function solution for a step change from some initial state x_{IS}, to a final state x_{FS}.

$$x(t) = x_{FS} - (x_{FS} - x_{IS})e^{-t/\tau}$$

Equation 2: A generalized step-function solution for a step change from initial state x_{IS} to a final state x_{FS}. x(t) is the time dependent response of the system, t is time, and τ is the time constant of the system. (Brock and Richardson, 2001)

Using Eq 2, if the initial and final temperatures of a step change are known and t is set to τ, then the equation can be solved to determine the value for x(t) at the time constant of the system. A plot of the raw data can then be created and the elapsed time required for any given system to reach this value is the time constant of the system. This is approximately equal to 63.2% of the total response.

To avoid differences between the systems due to different sensors, a Thermometrics (TMM) T5503 temperature sensor was placed inside the RM Young and the J-tube. This sensor has an accuracy of ±0.15 °C between -30 °C and 100 °C as per manufacturer specifications. Additionally, since the J-tube is typically used to measure RH as well as temperature (Straka et al. 1996), a Vaisala HMP35 Temperature and RH sensor was used inside the J-tube. This

unit specifies a temperature accuracy of ±0.04 °C on a range of -30 °C to 50 °C with 0.01 °C resolution (Straka et al. 1996). As a comparison for historical purposes, a Yellow Springs Inc. (YSI) 44018 Thermillinear Thermistor (also used in the original VORTEX project) was placed in the J-tube as well. This sensor has an accuracy of ±0.15 °C between -30 °C and 100 °C (Straka et al. 1996).

ii. Results

The initial starting temperature (x_{IS} in Eq 2) inside the vehicle bay was approximately 21.2°C, while the final temperature outside (x_{FS} in Eq 2) was 3°C. Using these numbers in Eq 2 and again setting $t = \tau$, x(t) will be approximately 9.88 °C at the time constant of each system. After completion of the test, the data was compiled and is plotted in Fig. 5.

The plot in the figure shows the large step change in tempearture as interpreted by each system according to their respective time constants. By examining the data, the elapsed time that the TMM sensor in the RM Young took to reach the calculated x(t) value was approximately 18 s. An identical sensor in the J-tube required an elapsed time 68 s to reach the same x(t), while the temperature sensor in the HMP35 took 5 min and 9 s to reach the same x(t) value.

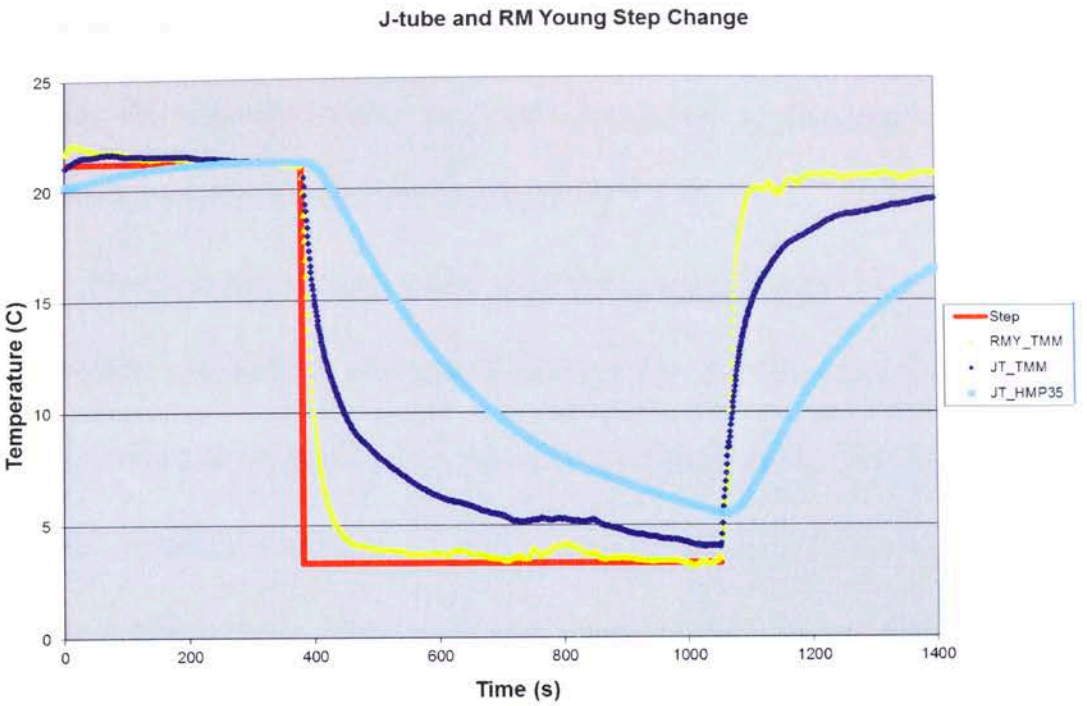

Figure 5: J-tube/RM Young response to a step change in temperature. The actual step change is depicted as a solid red line. Plot shows the TMM sensor in the RM Young (yellow diamond's), and the J-tube sensors: the TMM (blue diamond's), and the HMP35 (light blue 'x'). The time constant of the sensors are 18 s, 68 s, and 5 min 9 s respectfully, following the method outlined.

Thus, the same sensors in the two different shields will experience different time constants simply due to the difference between the shields. In this scenario, the TMM sensor in the RM Young is roughly four times faster than the TMM sensor in the J-tube, and is 17 times faster than the HMP35 sensor. Errors (greater than 3°C) occur between the J-tube and the RM Young simply due to these differences in the response time of the systems.

It is worth noting that were this scenario to occur in a real data collection period, the J-tube may severely dampen or even completely miss potentially large gradients in temperature. For example, if a change in temperature were to

occur during a period where the aspiration rate of the J-tube was being slowed (driving down the road with a tail wind), it may take a considerable amount of time for the sensors to reach the ambient temperature.

Furthermore, with the potentially slow response of the J-tube, if several gradients in temperature were encountered quickly, the J-tube may not reach the actual ambient air temperature in any particular environment. This may result in the true magnitude of the temperature change being underestimated. On a mobile platform, these gradients can be sampled rather quickly before moving into another airmass. The RM Young is, therefore, more suited to making fast response temperature measurements.

Chapter 5: Characterization Conclusions

After completion of the tests outlined in Section III, it was determined that the J-tube/RM Young combination would be acceptable for research applications involving the MMs. The J-tube is more reliable during rain, hail, and high winds from the front of the vehicle. The RM Young on the other hand is more accurate in low winds, high solar radiation, or varying wind directions. Each system has its own conditions where it performs well, and when combined the two systems cover most circumstances typically encountered by a MM. By

using both housings, at least one of the temperature shields should be performing correctly and would be able to be used for reliable temperature measurements. With this knowledge, the J-tube and the RM Young were put into use for the 2009 season of the VORTEX 2 project.

While the tests performed were vital and provided information to further characterize each shield, there were still some unanswered questions regarding the ability of each system to perform adequately. The J-tubes' response to high solar radiation values was still of concern as as the effectiveness of the RM Young during rain.

The downside to this arrangement is that both systems must be used simultaneously. This requires extra equipment to be mounted on a MM rack, an extra set of instruments, and a considerable cost to purchase the extra equipment. Furthermore, the RM Young was not intended to be repeatedly exposed to severe weather and tended to crack or break when hail was encountered, adding additional cost.

To further complicate the situation, extensive post processing is required of any data collected to determine when to use each system. In many cases this requires a manual analysis of several different parameters to determine the environmental conditions at the time and ultimately which shield to use. This is

both time consuming and tedious. As such, most end users (VORTEX 2) only want a single temperature shield.

With the completion of the initial experiments and the first year of VORTEX 2, it became readily apparent that there existed a need for a single temperature shield that would perform adequately in all possible situations that could be encountered on a MM. This shield would ideally combine the positive aspects of both the J-tube and the RM Young, but would reduce or eliminate as many of the drawbacks as possible. This new shield would be able to reduce the amount of equipment necessary to collect reliable temperature data over a wide range of scenarios and would ultimately allow the MM to safely be used in a broader spectrum of projects without fear of data quality issues.

To meet this need, a new temperature shield was to be designed, tested, and deployed prior to the start of the 2010 season of VORTEX 2.

Chapter 6: New Instrumentation: The U-tube

A. J-tube Modifications

Initially, when the decision to create a new shield was made, the primary focus was to simply modify the J-tube to be less directionally sensitive. The directionality of the J-tube is the single largest source of error in the system and it was thought that by eliminating it a more versatile shield could be created.

Simple and straightforward solutions such as adding a downward pointing exhaust were tested, and the findings were that in removing the directionality of the unit, the entire behavior of the system was altered. In most cases the unit failed to accelerate the aspiration rate with increasing speed since the pressure gradient that was driving the aspiration rate was now disrupted. Parallel plate structures on the exhaust were added to attempt to solve this problem, but the intake interfered with the system's ability to generate a strong enough pressure gradient to accelerate the flow rate.

In an attempt to solve this new issue, a change was made to the intake of the J-tube to try and make the system accelerate the flow more easily. Rather than have a horizontal intake, the J-tube was modified to simply have a vertical intake. With this now mostly vertical orientation, the J-tube's flow rate was slowed to around 1 ms^{-1} and no longer accelerated at all.

Variations on the intake were tried including an upward pointing, horizontal parallel plate structure. This resulted in a better response of the internal flow rate, but unfortunately resulted in rain easily being ingested into the system.

The complicating factor with these modifications was that while individual problems can be identified, it is extremely difficult to fix one problem without affecting another. A simple rule here per a personal conversation with

Sherman Fredrickson is that "There is always more than one thing influencing anything you are trying to measure." By attempting to solve a single problem on an existing instrument, more problems were being created or amplified.

As such it was decided that attempting to modify the existing J-tube was an endless spiral of possibilities with potentially no solution, and instead a new shield would be created from scratch. Several key features were identified from the previous trials that would be needed in order to assure that the new shield would have all the positive aspects of the J-tube/RM Young combination.

After identifying these features, there were several ways of implementing the respective designs. It was desired for the intake and the exhaust to be horizontal to maximize the airflow across the unit since this is the direction of the ambient wind. Those sections also needed to be downward facing to avoid any intake of water. There are several orientations of these features that can be achieved (both horizontal and vertical), but several tested either did not perform as desired or were overly complex in building and/or mounting. An inverted "U" shape was chosen as it was the most logical, non-interfering, functional design that met all the requirements necessary.

B. The U-tube

The U-tube is made from a combination of thin and thick walled schedule 40 PVC. There are three basic portions of the system: the intake, the

central housing, and the exhaust (Fig. 6). Any instruments used with the system are located in the central housing, as shown in the figure. The central housing is also large enough to allow the use of multiple sensors simultaneously. A small DC fan is located in the exhaust portion of the unit to provide a baseline airflow in the presence of no ambient wind. Additional images of the U-tube, showing its mounting on a MM, can be found in Appendix A, Figs. 2 and 3. For more detailed information regarding the construction, refer to Appendix B.

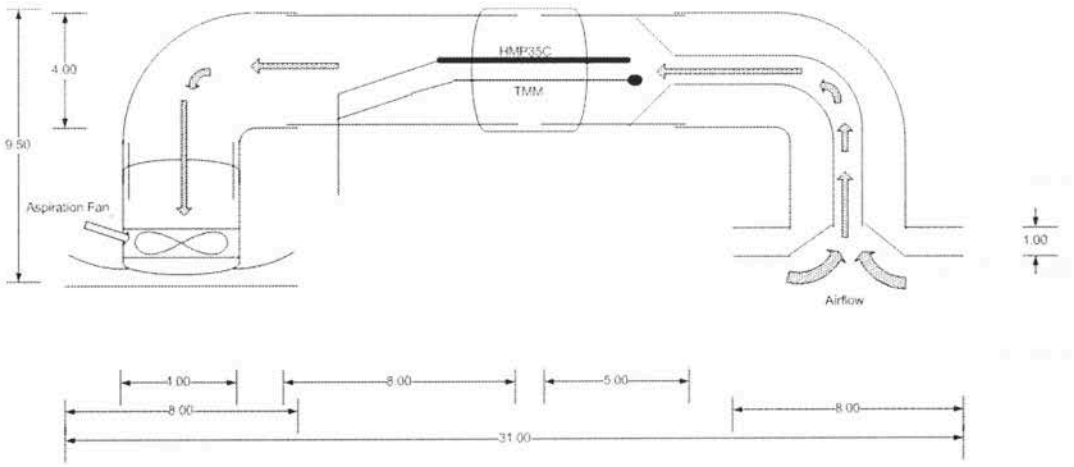

Figure 6: U-tube Schematic showing dimensions (in inches), airflow patterns, and instrument locations. The structure is made from a combination of thin and thick walled schedule 40 PVC and uses a small DC fan (30 ft^3/min) to help aspirate the unit in low wind conditions. The unit is intended to me mounted horizontally as shown with the intake (right) and the exhaust (left) pointing downwards toward the surface.

The intention of the U-tube was to provide an omni-directional, Bernoulli enhanced, temperature shield that protected any sensors used from solar radiation and rain. With this design, all of the major sources of error associated with temperature measurements on a mobile platform were addressed. Utilizing the features of the design, the shield should maintain

adequate exchange rates between the sensors and the outside air, as well as increase the ambient airflow rate as the vehicle travels at increasing speeds. For each section, the construction of the U-tube has a specific purpose such that the shape, orientation, and size of each piece plays a critical role in the ability of the U-tube to function properly.

i. Design and Features

a. The Intake

1. The Double Plate Intake

With the double plate system on the intake, the air that is being sensed originates from below the bottom plate. This reduces the up-flow thermal mass that the air must pass over before reaching the sensors and reduces any air mass modification. It also reduces the area that water may collect on, minimizing any wet-bulb errors that may occur.

The plates are symmetric so changes in the wind direction relative to the intake should not negatively affect its performance. Similar to a parallel plate structure used for making pressure measurements, the flat plates also help to streamline the flow, which in turn reduces any Bernoulli Effects that may be occurring (Antony et al. 2000). Proper air exchange is of concern and the flared intake on the lower plate helps to streamline the flow entering the instrument, increasing the aspiration rate. Since the opening on the bottom plate is not

covered, the unit is able to enhance the flow rate with any upward accelerations of air flow over the top of the vehicle when such air motions are present.

2. The Inner Tube

By using a second tube inside the main structure to provide the air flow to the sensors, they are effectively decoupled from any solar radiation effects on the outside of the shield. The insulating layer of air between the smaller inner tube and the larger outer tube will absorb (or emit) any energy transferred to (or from) it from the PVC walls through conduction, and is passed through the system without interacting with the sensors. Additionally, with the small diameter of the inner tube the ambient flow rate through the system is accelerated over the larger diameter of the outer tube (as compared to the J-tube which only has the larger diameter tube), and with a 30 ft^3/ min (0.014 m^3/s) fan, the ambient flow velocity that the sensors experience with no relative wind present is approximately 6 ms^{-1}.

3. The Downward Curve

The fact that the intake is pointing downward also provides crucial benefits to the system. Since the air is required to make an upward turn against gravity, any liquid water that is present in the air (i.e. rain drops), will be mechanically separated from the air stream as with the J-tube. Additionally, the

sensors are located far enough inside the structure that the curve prevents any solar radiation, whether direct or indirect, from interacting with the sensors.

b. The Central Housing

This section serves as a connection between the intake and the exhaust, and is used to house any temperature sensors needed. The number of sensors that the U-tube is capable of housing depends on the individual size of any particular sensor, but can easily accommodate two sensors. The interior size of the central housing allows these sensors to be mounted near the center of the shield, which removes them from conductive energy transfers near the outside wall and maximizes the airflow that reaches them.

c. The Exhaust

1. The Curved Double Plate

The exhaust section's double plate arrangement features a curved plate above a flat plate to induce a Bernoulli Effect that under increasing wind speed conditions creates a low pressure perturbation in the exhaust. This process is similar to what occurs over the vehicle roof while driving, and for an incompressible atmosphere is modeled by Eq 1. This sets up a pressure gradient between the intake and the exhaust (with a low pressure perturbation at the exhaust) that draws air through the U-tube and increases the aspiration rate of

the unit. As the wind speeds across the unit increase, the pressure gradient increases and consequently so does the aspiration rate. These plates are circular so that the exhaust is also omni-directional, as with the intake.

2. Downward Curved Structure

Similar to the intake, the exhaust is a downward pointing curved structure. This was done so that the double plate arrangement was horizontal to maximize the accelerations due to Bernoulli's Principle. As before, with this arrangement gravity is acting against any liquid water present and the DC fan is protected from wetting.

Chapter 7: Performance Testing

While the U-tube was created with the goal of fullfilling all the requirments of a mobile temperature system, testing was required to validate that the unit performed as desired. With the U-tube being an intended replacement for the J-tube/RM Young combination, all three shields were tested over a variety of circumstances to characterize the U-tube completely and answer any lingering questions surrounding the J-tube or the RM Young. The areas tested were solar radiation, wet bulb errors during rain, aspiration rate response to

changes in the relative wind speed/direction, and the overall time constant of the system.

A. Effects of Solar Radiation on Temperature Measurements

i. Experimental Setup

In order to test the units for potential errors during periods of high solar radiation, each unit needed to be placed in such an environment while making temperature measurements. While this is most easily accomplished on a hot summer day during peak solar heating with clear skies, performing this test in somewhat uncontrolled conditions is problematic. By placing the unit outside in the ambient air, often times the local temperature fluctuates on the order of +/- 2°C. Additionally, most other surfaces nearby are absorbing and reradiating energy from the sun, further complicating the test. Finally, during high solar heating, thermals are common, which adds to temperature fluctuations and results in changing wind conditions. These factors are all sources of error that can easily overpower any signal due to solar radiation alone and thus, make an outside test unreliable.

In order to perform the test in a more controlled environment, the testing facilities at EnvironLabs were used. This independent testing facility located in Minneapolis, MN specializes in environmental testing and is peridocally contracted by RM Young to test their equipment for solar radiation errors. Due

to its wide radiant spectrum output (Appendix A, Fig. 4) a metal halide lamp is used to reproduce solar heating (McPherson et al. 2007). After an intial warm up period, the 1000 W lamp produces a solar equivalent of 950 W/m^2 at a distance of approximately 31 inches (787.4 mm) over an circular area of approximately 15 inches (381 mm) in diameter. The intensity of the light in this area is assumed to be uniform. The large bay area at EnvironLabs where the tests were performed was large enough so that heat generated from the lamp would not be introduced into the temperature shields, resulting in error.

During the test, each shield was placed in the light at several angles and orientations in order to determine how any solar radiation errors vary with incidence angle. The angles used were straight on from the side (0°), 45° on the side, straight on top of the unit (90°), 45° on the front, and straight on from the front (0°) (see Figure 7 for example diagram). During each run, the unit was left in the solar lamp for 30 minutes. After each period of measurements were made, the unit being tested was removed from the light and allowed to cool back to ambient temperature.

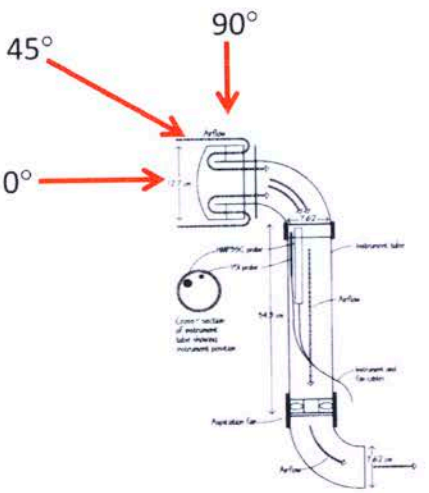

Figure 7 : Side view of J-tube depicting solar radiation angles of 0, 45, and 90° tested from the 'front' of the J-tube. The 'side' angle are the same, but are pointing into the page looking at the J-tube in this orientation. A similar arrangement was used for the U-tube.

The temperatures inside each shield were measured using a TMM sensor. For the tests, the RM Young was used as the reference (Hubbard et al. 2005, Richardson et al. 1999, Anderson et al. 1998, Brandsma and Vander Meulen 2008).

ii. Results

When exposed to solar radiation, both the J-tube and the U-tube tend to experience an error (Fig. 8). During the tests, the J-tube experienced a maximum error of approximately 1.1°C (occurring at the 0° from the side sun angle) and showed sensitivity to the direction of the incoming solar radiation with the maximum errors occurring at low sun angles (0° angle). The U-tube experienced a maximum difference (when compared to the RM Young) of only 0.6°C (occurring at the 0° from the side sun angle) and was also slightly sensitive to the sun angle (less than 0.3°C change). The errors shown on Fig. 7 are the maximum errors obtained after a 30 min. exposure. It is also important that during the tests the J-tube began to show a noticeable increase in temperature after approximately 5 min. of solar radiation exposure while the U-tube took much longer (typically 20 min.) to show a similar change in temperature.

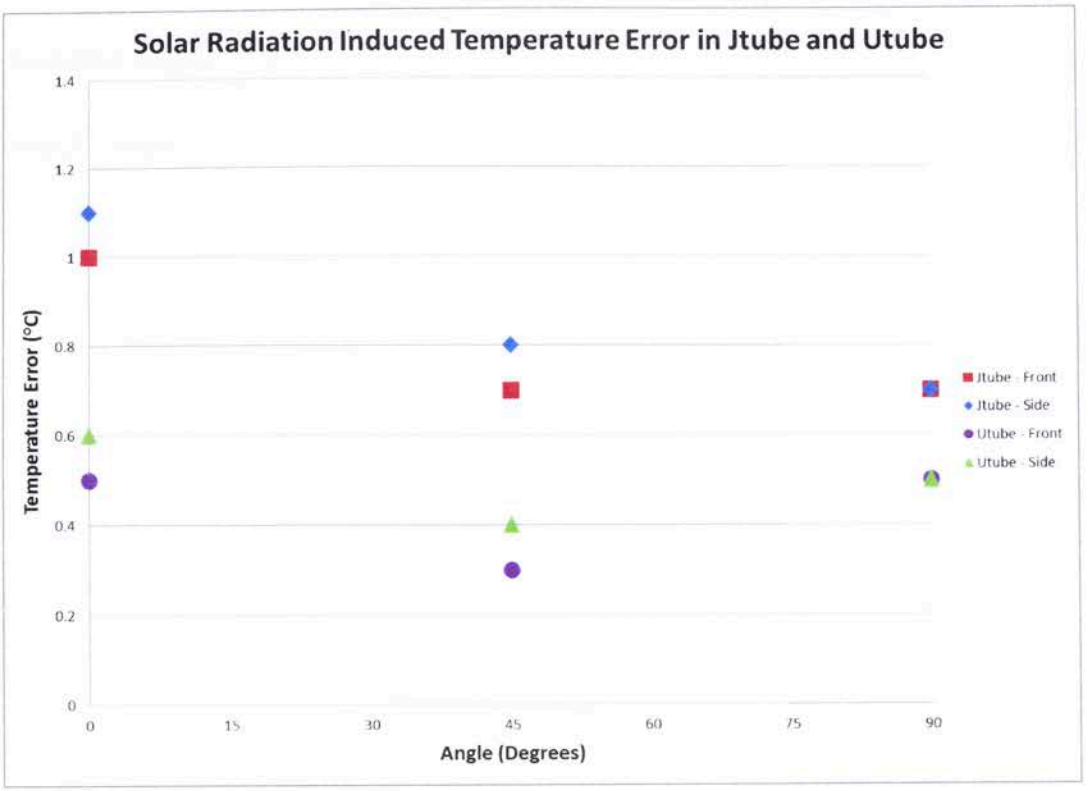

Figure 8: Solar Radiation induced temperature errors (°C) for the U-tube and J-tube after 30 min exposure to 950 W/m^2 solar radiation over various angles. The errors shown represent the maximum error achieved after the 30 min exposure to the radiation. Both systems show a tendancy to increase their error with lower (more horizontal) sun angles.

The results of this test indicate that the J-tube is likely to experience errors when used in situations with high solar radiation. Furthermore, since the J-tube was quicker to respond once the solar lamp was applied, these errors will begin to become problematic quickly. The U-tube is better able to handle the high solar radiation values by producing less error than the J-tube, and taking longer to show that error.

However, since these shields will be used on a mobile platform one must consider the effect of a reflective surface nearby. The solar test only examined situations where incoming solar radiation was from a single direction. If

mounted above a reflective car roof, additional solar radiation may be present which could increase the magnitude of any errors. While the RM Young is commonly used as a reference for solar radiation, it is done so in situations where the incoming solar radiation is directed from above. Due to the proximity of the temperature sensor to the intake, reflected radiation from directly below the unit could result in direct solar heating of the sensor and large temperature errors.

B. Effects of Rain on Temperature Measurements

i. Experimental Setup

To test the three shield's behavior during rain events, all three systems were put through several iterations of wet and dry conditions. Rather than trying to recreate such an environment, a data set from the 2010 season of the VORTEX 2 project was used. Prior to the beginning of the second phase of the project, the U-tube was installed alongside the J-tube and the RM Young on all seven of the NSSL MMs. This was done to provide a comprehensive data set over the duration of the project from which the three systems could be compared in a variety of situations.

Following the completion of the project, data from all the MMs were examined to identify potential areas for analysis. The data set chosen was from Probe 2 during operations on May 10th, 2010. This collection period was

characterized by several periods of rain and was examined for differences between the various instruments. All three temperature shields had the same sensors (TMM) in use.

ii. Results

A plot of the 1 second, raw temperature records from the J-tube, the RM Young, and the U-tube during the period is shown in Figure 9. Note that at the beginning of the period, the 3 radiation shields agree, within the specifications

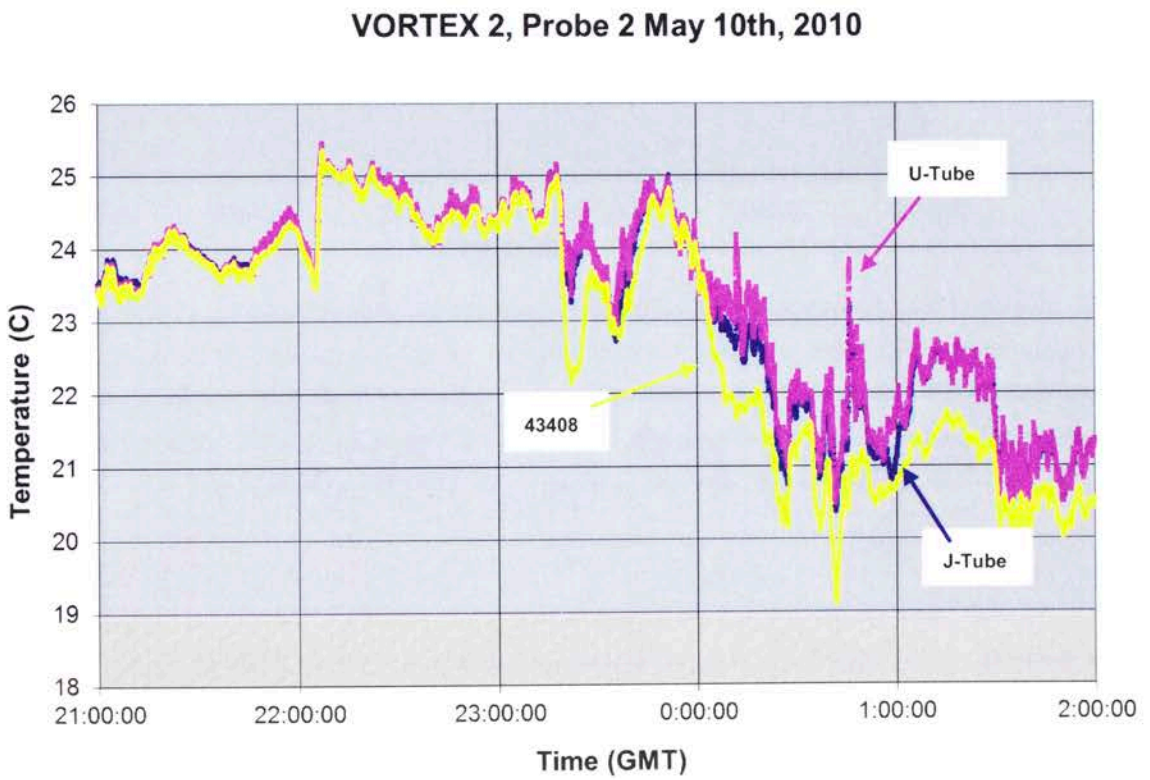

Figure 9: Temperature trace for Probe 2 during VORTEX 2 on May 10th, 2010. Data collection period is characterized by several periods of rain, during which the 43408 shows colder temperatures than either the J-tube or the U-tube. At the beginning of the period, before the rain events, all three systems agree.

of the instruments. Figure 10 shows a difference plot, using the U-tube as a reference, of the same data in Figure 9.

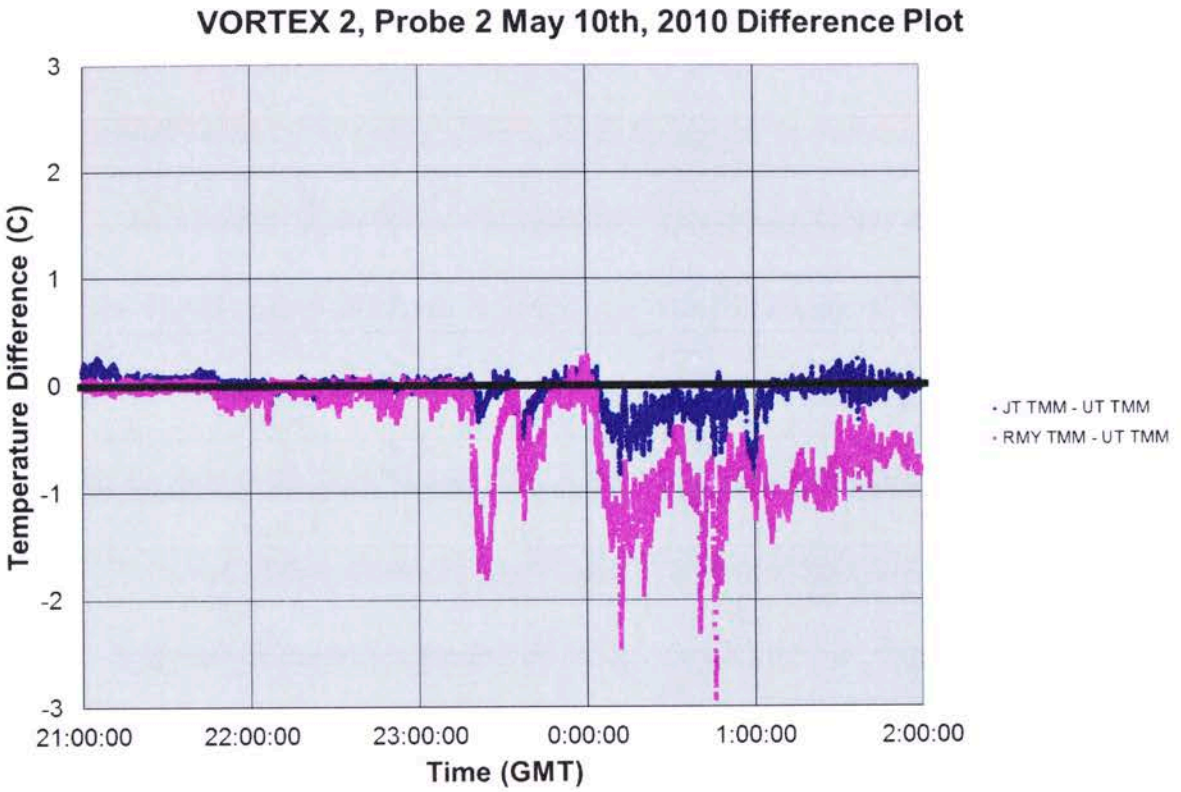

Figure 10: Difference plot of the temperature data shown in Figure 9, using the U-tube as a reference. The departure of the J-tube TMM sensor from the U-tube TMM sensor (JT TMM - UT TMM) is shown in dark blue while the departure of the RMY TMM sensor from the U-tube TMM sensor (RMY TMM – UT TMM) is shown in light purple. Initially, all three systems agree, however later in the period the RM Young and the J-tube show lower temperature readings than the U-tube, which is caused by wet-bulb effects.

The first instance of rain is encountered near 23:15:00 UTC. Periods of rain were determined through a combination of operator comments, proximity to radar echoes, and relative humidity changes. Once this period of rain is encountered, all three temperature shields show a noticeable decrease in temperature; however the RM Young continued to cool past either the J-tube or

the U-tube. This behavior is noted several times during this period with each difference occurring during and immediately following periods of rain. Since the sensors only disagree after rain is encountered, it is concluded that the differences between the systems are most likely caused by wet-bulb errors.

This source of error is consistent with the types of errors documented by Van der Meulen and Brandsma in 2008, and with the design of the RM Young. While the proximity of the temperature sensor to the opening and the high aspiration rate of the RM Young allows for a faster response time of the unit, it also allows the system to easily ingest rain. The sensor becomes saturated and once evaporation begins, temperature errors result. In one instance, the RM Young read nearly 3°C lower than the U-tube. The RM Young is, therefore, not suited for use in situations where rain is possible.

Overall the U-tube read the warmest throughout the multiple events, indicating that it was the least influenced by wet-bulb errors. While the J-tube was close to the U-tube, there were a few brief periods where the J-tube read slightly cooler than the U-tube (ex. 00:50:00 UTC). These situations however only appeared after rain had been encountered for longer than 10 min., indicating that water is able to eventually work its way into the J-tube and lead to errors.

The U-tube and J-tube were examined periodically throughout the project to determine if water was able to work its way into the system. This is evident on the interior of the unit due to the presence of water streaks on the interior walls of the shields. As the units are exposed to the outside air, dirt and dust are collected on the walls of the temperature shields. If rain is able to be ingested into the system, this water will essentially wash off areas of the interior walls, leaving streaks in the dust which indicate that water was present. Examining the J-tube after several rain events encountered on VORTEX 2: 2010, the temperature shield showed several of these streaks while the U-tube did not.

C. Response to Changes in the Relative Wind Speed/Direction

i. Experimental Setup

In order to determine the ability of the U-tube to be omni-directional, a modified MM from the VORTEX 2 project was used. Rather than simply repeating the previous experiment that was done to test the J-tube and the RM Young, a new test was designed that would determine the response of the shields without the influence of the vehicle. This was done due to concerns about the sensitivity of the placement of the J-tube. As was discussed previously, the J-tube relies on its proximity to the car roof to function properly. Since many groups are using the shield in locations other than directly above the vehicle

(examples include Karstens et al. 2010, Taylor et al. 2011, Skinner et al, 2011, Lee et al. 2011), it was desired to determine the response of the shield alone.

The modified MM had the U-tube and the J-tube mounted as high above the vehicle as possible without running into clearance issues (about 7 ft. [2.1 m] above the vehicle for a total height of approximately 13ft [4 m] above ground). At this height, the slipstream of the vehicle could be safely neglected and the response of each unit would be due only to the design of the shield. Both the J-tube and the U-tube were mounted on this MM in such a way that allowed the units to be rotated a full 360°.

This test would need to be modified depending on the type of vehicle used. The blockier the vehicle, the higher above the vehicle one would need to be in order to be free of the turbulence created by the vehicle. The Dodge Grand Caravan that the MM rack was mounted on is a fairly streamlined vehicle, as compared to a blunter vehicle such as a cargo van. One would ultimately need to test any vehicle intended to be used to determine at what height acceptable measurements could be made. This was done previously on the NSSL MMs by making wind measurements at various heights above the vehicle using cup anemometers. The tests showed that the height chosen for the mounting of the J-tube and U-tube would remove the shields from any significant influence of the vehicle.

Similar to what was done before, the MM was taken out at night to the "Ten Mile Flats" area during calm conditions. The MM was then driven at speeds of 10 mph, 20 mph, 40 mph, and 60 mph (4.5, 8.9, 17.9, and 26.8 ms^{-1} respectfully) with the units mounted in their original mounting orientations. The units were then rotated 45° counter-clockwise and the runs repeated until a full 360° rotation had been achieved. As before, a hot wire anemometer was used to measure the internal flow rate in each shield. By driving the vehicle in calm conditions with the shields mounted at various angles, the test effectively created a controlled relative wind for specific angles to the shields.

ii. Results

With no ambient wind present, the U-tube has a flow speed of approximately 6 ms^{-1}, as compared to the 1.5 ms^{-1} ambient flow speed of the J-tube. The behavior of these two systems to changes in the relative wind was compiled and is shown in Fig. 11. First consider only the response due to changes in the relative wind direction, and then consider how those changes are magnified by the relative wind speed.

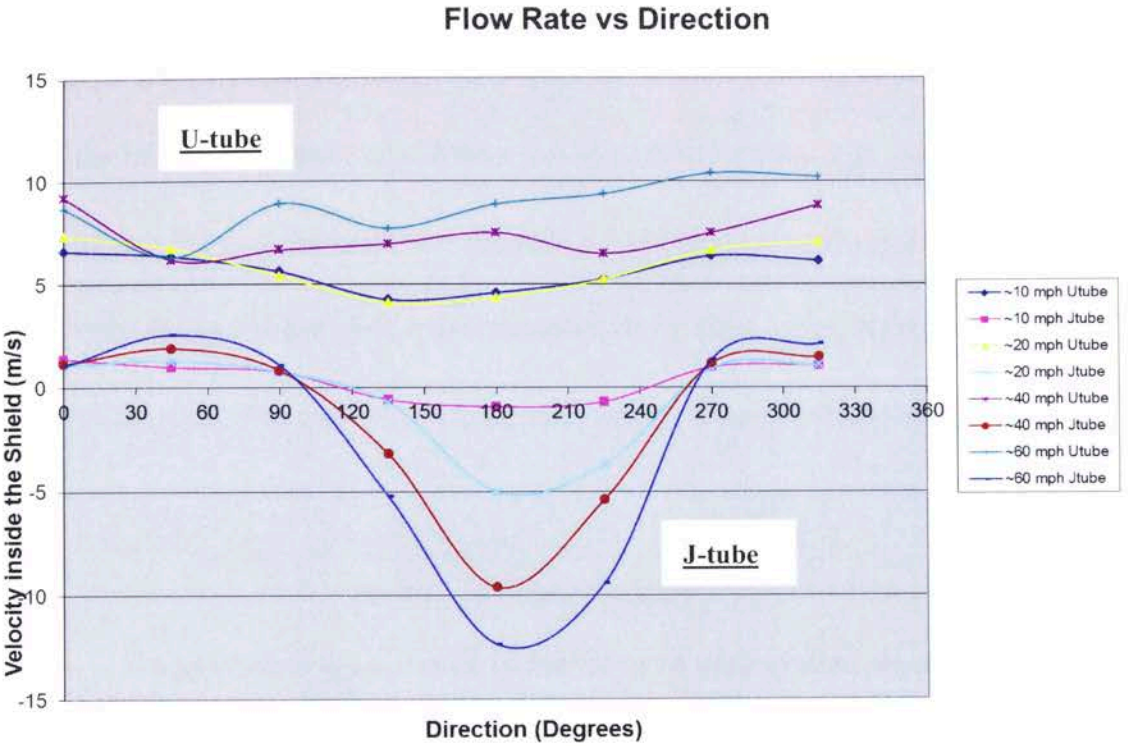

Figure 11: Sensitivity of the U-tube and J-tube's flow rate to varying relative wind direction angles (horizontal axis), shown are 10, 20, 40, and 60 mph wind speeds. Flow rate through both systems is shown on the left axis. Graph indicates the J-tube's sensitivity to the relative wind and its tendency to decrease its flow rate to the point of reversing directions when the flow approaches the rear of the J-tube. This is magnified with increasing wind speeds. Graph also shows the sensitivity of the U-tube, and its tendency to generally increase the flow with increasing wind speeds.

a. Relative Wind Direction

Examining the 10 mph (4.5 ms^{-1}) case, the J-tube is still directionally sensitive as was found before. When the relative wind approaches the rear of the J-tube, the aspiration rate slows down and eventually reverses directions.

The U-tube, on the other hand, has only a slight variation in aspiration rate with changes in the relative wind direction. While both the intake and the exhaust are omni-directional by design, they are somewhat in line with each

other (the exhaust is slightly lower than the intake is). As such, turbulence off one or the other can influence the piece downwind, resulting in a reduced ability of the unit to accelerate the airflow into the intake and through the exhaust. This reduction in performance in minimal (3 ms^{-1} change) and does not affect the overall ability of the unit to maintain positive flow rates. Next consider how these directional sensitivities are altered with increasing wind speeds.

b. Relative Wind Speed

In general, the directional sensitivities of each system are magnified with increasing speeds. The J-tube is particularly sensitive to this with the rearward components of the wind. At 60 mph (26.8 ms^{-1}) relative wind speed over the vehicle directed at the rear of the J-tube, the aspiration rate inside the J-tube is approaching 12 ms^{-1} backwards. This behavior is similar to what was discovered previously. Of particular significance is the lack of accelerated flow rates when the relative wind is from the front of the J-tube, as was the case before when it was mounted near the roof of the vehicle. This indicates that the J-tube is only able to accelerate airflow through the system when placed close enough to the roof of the vehicle to make use of the accelerated airflow over the roof. When mounted away from this air stream (while still pointed into the direction of the relative wind), the J-tube is unable to accelerate the airflow on its own and maintains a relatively constant flow rate despite the increasing relative winds.

Conversely the U-tube increases its aspiration rate with the increasing relative wind speed, despite the direction of the relative wind. Overall the omni-directional design of the U-tube is able to continue to increase the flow speed by continuously accelerating the airflow through the curved stacked plates, inducing a stronger PG and consequently a stronger flow rate. A maximum flow speed of 10 ms^{-1} occurs at 60 mph (26.8 ms^{-1}). While its response isn't entirely symmetric, the aspiration speed at a minimum maintains; it never decreases.

D. System Time Constant

i. Experimental Setup

The base time constants for the J-tube and the RM Young (both with TMM sensors installed) were already known at this point, but the test was repeated to determine the U-tube's time constant and how it compared to the other systems. The same experiment as was described in Section IV.C.i was used, except modified to additionally contain a U-tube temperature shield. As with the other two systems, the U-tube used a TMM temperature sensor in order to maintain comparability between the systems. In order to further examine the characteristics of the HMP35 sensor used in the J-tube, an additional HMP35 sensor was placed in the U-tube during the test.

ii. Results

The temperature traces for the three shields and their respective sensors are shown in Fig. 12. In this test, the initial temperature was 20.5°C (x_{IS} in Eq 2) and the final temperature was 2.5°C (x_{FS} in Eq 2). As before, if we set $t = \tau$ in

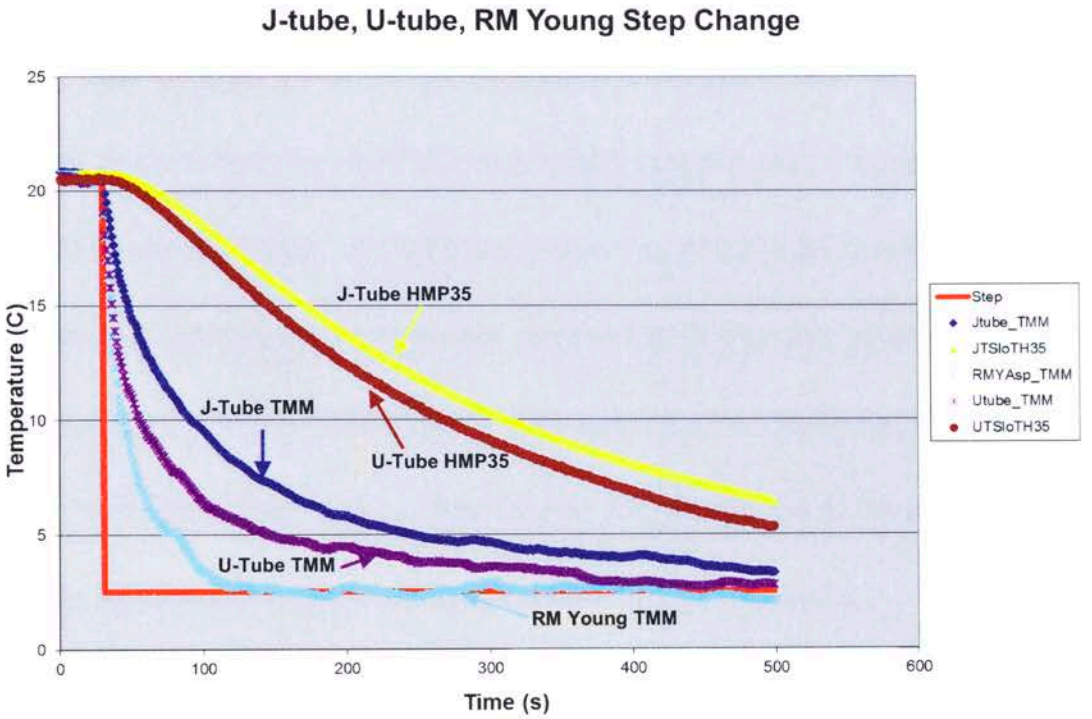

Figure 12: Temperature shields response to a step change in. Actual step change shown as a solid red line. Time constants for the TMM sensors are 18 s, 33s, 76 s for the RM Young, U-tube, and J-tube respectfully. The U-tube HMP35 had a time constant of 4 min 28 s while the J-tube HMP35 had a time constant of 5 min 16 s.

Eq 2, then we can solve the equation for x(t), which is the value that a system will have at after an elapsed time equal to the systems time constant. Performing these calculations, we find that $x(t) = 9.2°C$ when $t = \tau$. Examining the data in Figure 12, we find that for the TMM sensors the J-tube took 76 seconds to reach the x(t) value, the U-tube required 33 seconds of elapsed time to reach the same x(t), and the RM Young required only 18 seconds to do the same.

As was the case before, the RM Young is still the fastest to respond to a change in temperature, followed by the U-tube, with the J-tube being the slowest to respond. Errors in excess of 3°C occurred between the J-tube and the U-tube simply because of time constant differences.

One can also examine the differences in response time of the HMP35 sensors. In the J-tube, the HMP35 sensor took 5 minutes and 16 seconds to reach the indicated x(t) value. An identical sensor in the U-tube required only 4 minutes and 28 seconds to reach the same point. While still slow to respond when compared to the TMM, the U-tube increased the response time of this sensor over the J-tube. When compared to the J-tube, the U-tube is a more reliable temperature shield when used in calm, benign conditions.

Chapter 8: Conclusions and Remarks

The J-tube's design makes it sensitive to changes in the relative wind speed and direction, while its slow response time will make any temperature gradients sampled appear much smoother and more drawn out than in reality. As was defined earlier, this would be a gradient dampener. Additionally, its use in situations involving high values of solar radiation results in errors, which was cautioned against by Straka et al, 1996. The U-tube does not have these

directional sensitivities and is much faster to respond to changes in temperature while simultaneously reducing errors associated with solar radiation.

The RM Young works well during most non-severe conditions and has an advantage in base response time over the U-tube, however, its tendency to produce wet bulb errors during rain events and its susceptibility to hail makes the unit's use in convective weather research problematic. Furthermore, since the RM Young does not alter its aspiration rate positively with changes in the relative wind direction or speed as with the U-tube, the RM Young will be slower to mix with the ambient air at high vehicle speeds. The increased aspiration of the U-tube at these higher speeds allows the unit to continue to sample the environment as quickly as possible while driving.

When used in together, the J-tube and the RM Young will cover most commonly encountered situations, but there will still exist scenarios where both systems may have potential problems. Additionally, the use of both systems in conjunction would require a user to examine the data carefully to determine at which points to use which system: a very time consuming, complicated, and tedious task. The U-tube eliminates this requirement and the need for a second set of instruments, by combining all of the positive features of the J-tube/RM Young into a single unit. The U-tube is robust enough to withstand the harsh

environments of severe weather while meeting all of the necessary requirements for scientific research.

After the U-tube was mounted on all seven of the NSSL MM's, several of them were used for a variety of field projects that allowed the comparison of several data sets with all three systems in use. These data sets cover a wide range of conditions and provide a long term comparison between the systems. The entire 2010 season of VORTEX 2, as well as a deployment to Hurricane Irene 2011, were examined.

A. VORTEX 2: 2010

After completion of the second year of VORTEX 2, it was determined that in all cases the U-tube performed either equal to, or better than, the J-tube/RM Young combination. When conditions existed that caused either the J-tube or the RM Young (or both) to experience difficulties, the U-tube responded positively.

Furthermore, since VORTEX 2 was a severe weather research project, hail was commonly encountered. While most of this hail was small, several instances of baseballs or larger occurred. Neither the J-tube nor the U-tube suffered any performance affecting damage to the radiation shield in any of the hail encountered. The RM Young however, tended to crack or break in several places, forcing parts of the system to be replaced frequently.

B. Hurricane Irene

In August 2011, a MM was taken to North Carolina for a brief deployment on Hurricane Irene. This provided an opportunity to examine the three temperature shields over an extended period of wind driven rain. During the deployment, winds in excess of 70 mph (31.3 ms^{-1}) and heavy rain were commonly encountered. Examining the data from the shields, the RM Young consistently read cooler than either the J-tube or the U-tube as it continued to have problems ingesting water.

Additionally, the varying wind direction tended to cause problems with the J-tube; most notably by ingesting water into the system through the exhaust. This case provides further proof of the U-tube's ability to respond positively in a large variety of environments.

C. Regarding the J-tube's previous use

Prior to the U-tube, the NSSL MMs have made use of the J-tube since its inception in 1994. With the revelation of the J-tube's drawbacks, there arises the possibility that in previous data collection efforts, the J-tube may have been used in environments where the J-tube has now been shown to produce errors. However, the location of the J-tube atop the NSSL MMs has provided a unique environment that allowed the J-tube to function in a semi-acceptable manner. On

NSSL's instrument racks, the J-tube is placed in close proximity to the vehicle roof.

As has been previously discussed, this arrangement allows the J-tube to take advantage of the acceleration over the vehicle roof and accelerate the aspiration rate inside the unit. In effect, the vehicle itself is creating a Bernoulli process that the J-tube is able to use to increase its aspiration rate as the vehicle moves faster. The J-tube still has the solar radiation and directional sensitivity, but does increase its aspiration rate with increasing relative wind speeds from the front of the unit. As long as the vehicle is in motion and not in high solar radiation, the J-tube is much more likely to function properly.

There still exist potential scenarios while moving that could result in a rearward component to the relative wind as mentioned earlier. Previous data collected that is questionable should therefore be examined to determine if any of these situations are occurring, and those periods of data carefully examined for potential errors.

By placing the J-tube in a different orientation or location, by placing it atop a different vehicle other than those used by NSSL in the past, or by changing the design of the shield and/or the instrument rack, the behavior of the J-tube cannot be guaranteed to work as intended. Many more considerations,

such as any potential directionality issues or any nearby accelerated airflows, must be made in order to use the J-tube appropriately.

The U-tube is much more versatile and is not as sensitive to placement and other factors. This makes the U-tube applicable to a variety of mobile platforms with several types of demands and applications. The author recommends that the U-tube be used from this point forward for mobile temperature measurement applications.

References

Anderson, Steven P., Mark F. Baumgartner, 1998: Radiative Heating Errors in Naturally Ventilated Air Temperature Measurements Made from Buoys*. *J. Atmos. Oceanic Technol.*, **15**, 157–173.

Brandsma, T. and Van der Meulen, J. P. 2008, Thermometer screen intercomparison in De Bilt (the Netherlands)—Part II: description and modeling of mean temperature differences and extremes. International Journal of Climatology, 28: 389–400.

Brasefield, C. J., 1948: Measurement of Air Temperature in the Presence of Solar Radiation. *J. Meteor.*, **5**, 147–151.

Brock, Fred V., Kenneth C. Crawford, Ronald L. Elliott, Gerrit W. Cuperus, Steven J. Stadler, Howard L. Johnson, Michael D. Eilts, 1995: The Oklahoma Mesonet: A Technical Overview. *J. Atmos. Oceanic Technol.*, **12**, 5–19.

Brock, Fred V., Scott J. Richardson (2001). "Meteorological Measurement Systems", Oxford University Press, New York, 290 pp.

Buban, Michael S., Conrad L. Ziegler, Erik N. Rasmussen, Yvette P. Richardson, 2007: The Dryline on 22 May 2002 during IHOP: Ground-Radar and In Situ Data Analyses of the Dryline and Boundary Layer Evolution. *Mon. Wea. Rev.*, **135**, 2473–2505.

Fuchs, M., C. B. Tanner, 1965: Radiation Shields for Air Temperature Thermometers. *J. Appl. Meteor.*, **4**, 544–547.

Grzych, Matthew L., Bruce D. Lee, Catherine A. Finley, 2007: Thermodynamic Analysis of Supercell Rear-Flank Downdrafts from Project ANSWERS. *Mon. Wea. Rev.*, **135**, 240–246.

Hirth, Brian D., John L. Schroeder, Christopher C. Weiss, 2008: Surface Analysis of the Rear-Flank Downdraft Outflow in Two Tornadic Supercells. *Mon. Wea. Rev.*, **136**, 2344–2363.

Hubbard, K. G., X. Lin, C. B. Baker, B. Sun, 2004: Air Temperature Comparison between the MMTS and the USCRN Temperature Systems. *J. Atmos. Oceanic Technol.*, **21**, 1590–1597.

Hubbard, K. G., X. Lin, C. B. Baker, 2005: On the USCRN Temperature System. *J. Atmos. Oceanic Technol.*, **22**, 1095–1100.

Joseph, Antony, J. A. Erwin Desa, Peter Foden, Kevin Taylor, Jim McKeown, Ehrlich Desa, 2000: Evaluation and Performance Enhancement of a Pressure Transducer under Flows, Waves, and a Combination of Flows and Waves*. *J. Atmos. Oceanic Technol.*, **17**, 357–365.

Karstens, Christopher D., Timothy M. Samaras, Bruce D. Lee, William A. Gallus, Catherine A. Finley, 2010: Near-Ground Pressure and Wind Measurements in Tornadoes*. *Mon. Wea. Rev.*, **138**, 2570–2588.

Lang, Timothy J., and Coauthors, 2004: The Severe Thunderstorm Electrification and Precipitation Study. *Bull. Amer. Meteor. Soc.*, **85**, 1107–1125.

Lee, Bruce D., Catherine A. Finley, Timothy M. Samaras, 2011: Surface Analysis near and within the Tipton, Kansas, Tornado on 29 May 2008. *Mon. Wea. Rev.*, **139**, 370–386.

Lin, X., Kenneth G. Hubbard, George E. Meyer, 2001a: Airflow Characteristics of Commonly Used Temperature Radiation Shields*. *J. Atmos. Oceanic Technol.*, **18**, 329–339.

Lin, X., K. G. Hubbard, E. A. Walter-Shea, J. R. Brandle, G. E. Meyer, 2001b: Some Perspectives on Recent In Situ Air Temperature Observations: Modeling the Microclimate inside the Radiation Shields*. *J. Atmos. Oceanic Technol.*, **18**, 1470–1484.

Markowski, Paul M., 2002a: Hook Echoes and Rear-Flank Downdrafts: A Review. *Mon. Wea. Rev.*, **130**, 852–876.

Markowski, Paul M., 2002b: Mobile Mesonet Observations on 3 May 1999. *Wea. Forecasting*, **17**, 430–444.

Markowski, Paul M., Jerry M. Straka, Erik N. Rasmussen, 2002: Direct Surface Thermodynamic Observations within the Rear-Flank Downdrafts of Nontornadic and Tornadic Supercells. *Mon. Wea. Rev.*, **130**, 1692–1721.

McPherson, Renee A., and Coauthors, 2007: Statewide Monitoring of the Mesoscale Environment: A Technical Update on the Oklahoma Mesonet. *J. Atmos. Oceanic Technol.*, **24**, 301–321.

Pietrycha, Albert E., Erik N. Rasmussen, 2004: Finescale Surface Observations of the Dryline: A Mobile Mesonet Perspective. *Wea. Forecasting*, **19**, 1075–1088.

Nakamura, Reina, L. Mahrt, 2005: Air Temperature Measurement Errors in Naturally Ventilated Radiation Shields. *J. Atmos. Oceanic Technol.*, **22**, 1046–1058.

Richardson, S. J., 1995: Multiplate radiation shields: Investigating radiational heating errors. Ph.D. thesis, University of Oklahoma, 133 pp.

Richardson, Scott J., Fred V. Brock, Steven R. Semmer, Cathy Jirak, 1999: Minimizing Errors Associated with Multiplate Radiation Shields. *J. Atmos. Oceanic Technol.*, **16**, 1862–1872.

Rodi, A. R., P. A. Spyers-Duran, 1972: Analysis of Time Response of Airborne Temperature Sensors. *J. Appl. Meteor.*, **11**, 554–556.

Shabbott, Christopher J., Paul M. Markowski, 2006: Surface In Situ Observations within the Outflow of Forward-Flank Downdrafts of Supercell Thunderstorms. *Mon. Wea. Rev.*, **134**, 1422–1441.

Skinner, Patrick S., Christopher C. Weiss, John L. Schroeder 2011: Observations of the surface Boundary Structure within the 23 May, 2007 Perryton, Texas Supercell. *Mon. Wea. Rev.*, e-View only attm.

Stonitsch, John R., Paul M. Markowski, 2007: Unusually Long Duration, Multiple-Doppler Radar Observations of a Front in a Convective Boundary Layer. *Mon. Wea. Rev.*, **135**, 93–117

Straka, Jerry M., Erik N. Rasmussen, Sherman E. Fredrickson, 1996: A Mobile Mesonet for Finescale Meteorological Observations. *J. Atmos. Oceanic Technol.*, **13**, 921–936.

Taylor, Neil M., and Coauthors, 2011: The Understanding Severe Thunderstorms and Alberta Boundary Layers Experiment (UNSTABLE) 2008. *Bull. Amer. Meteor. Soc.*, **92**, 739–763.

Appendix A: Additional Figures

Figure 1: Cart mounted rack created for time constant study. Rack pictured shows mounting of RM Young Wind Monitor, J-tube, and RM Young 43408. The orientations of the instruments are the same as is used on the Mobile Mesonet. The cart used for the U-tube portion of this test was identical to the cart pictured above, except with the U-tube mounted to the side of the J-

Figure 2: Mobile Mesonet showing mounting location and orientation of the U-tube. The picture was taken from the nose of the vehicle. The intake is on the passengers (left) side of the vehicle while the exhaust is on the drivers (right) side. The mounting location puts the U-tube above the front windshield to maximize airflow without distortions from the rack, but is high enough to be removed from reradiation of energy off the vehicle roof.

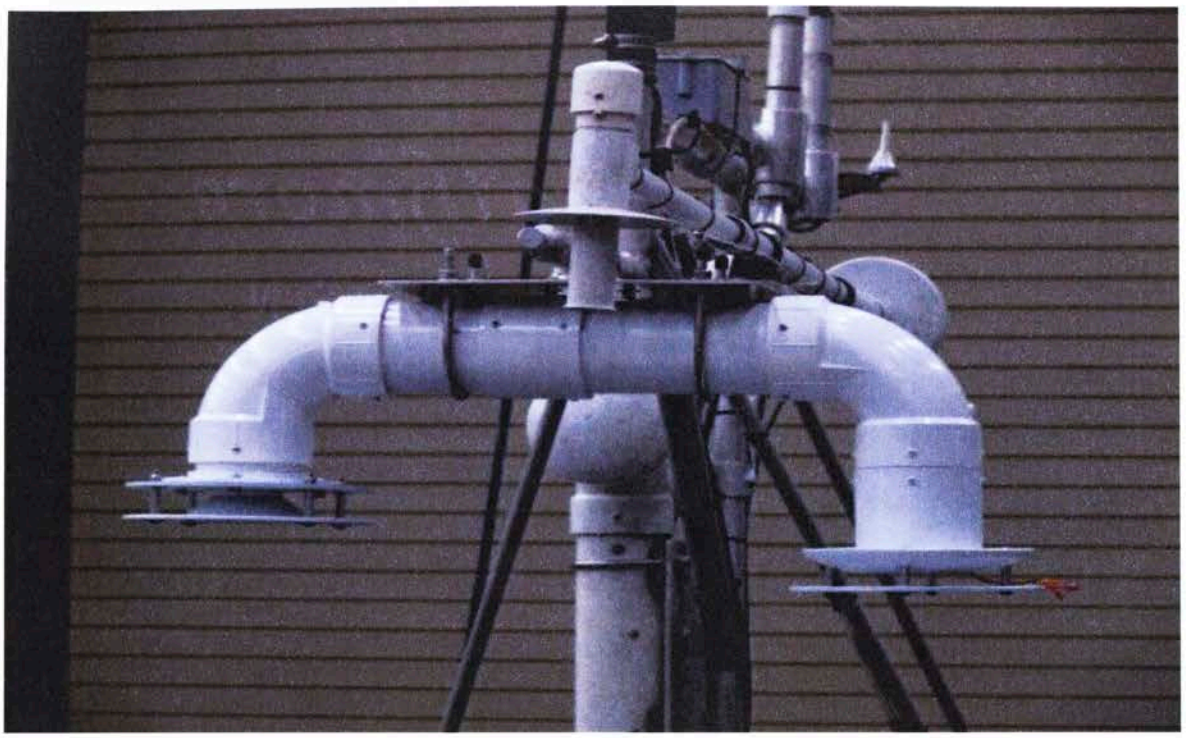

Figure 3:Close up view of the U-tube as shown in Fig. 2.

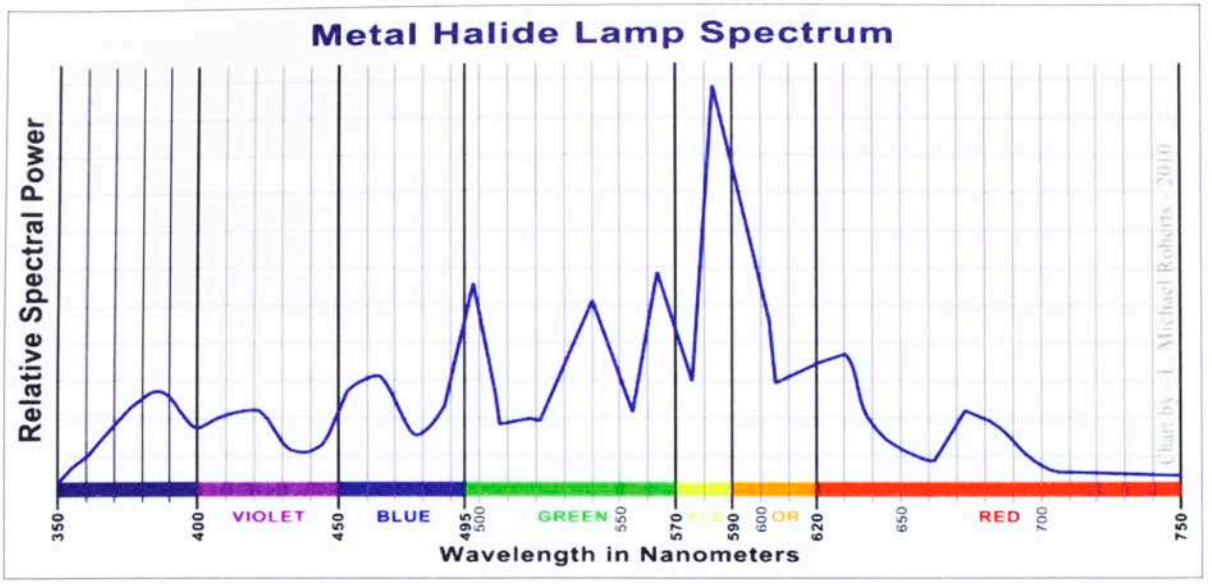

Figure 4: Radiant spectrum of a metal halide lamp. Due to the wide spectrum, this type of lamp is used to reproduce a solar spectrum for environmental testing purposes as the lamp produces radiation in the ultra-violet range.

Figure 5: Close up image of the intake section of the U-tube. The intake features two parallel plates as shown and a funnel attached to the lower plate.

Figure 6: NDS PVC adapter modified for use in making funnel by cutting off the larger circular section.

Figure 7: Lasco SCH40 45° Elbow. This elbow makes a 90° corner, but does so slowly across the curve rather than a sharp corner.

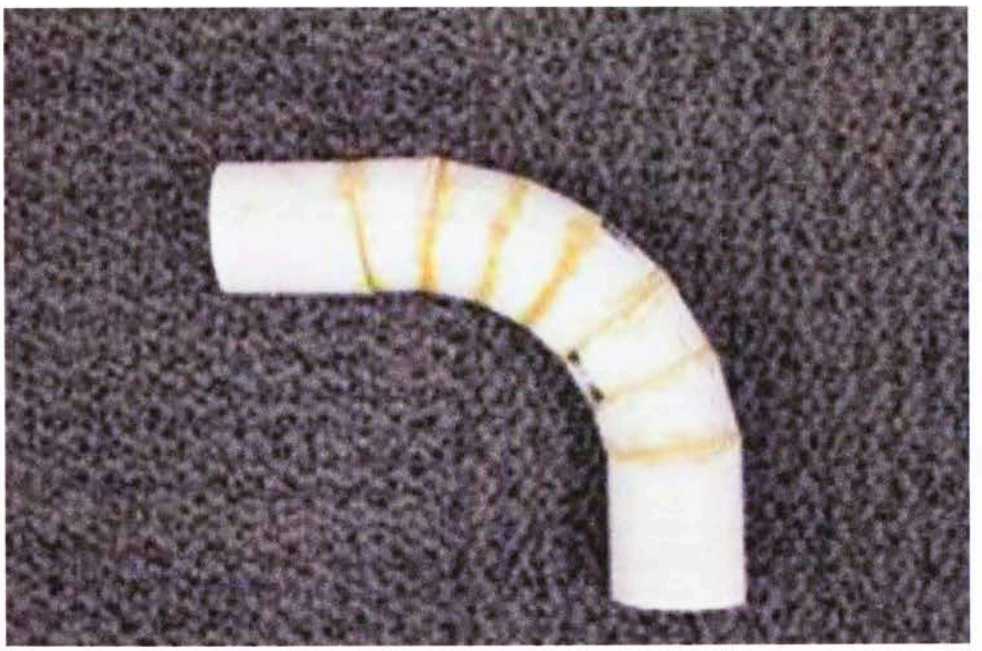

Figure 8: Inner tube created by piecing several sections of 1 inch (25.4 mm) diameter tube. Each section was created from a straight pipe cut at opposing 7.5° angles.

Figure 9: Image depicting the attachment of the inner tube to the funnel on the intake. The inner tube curves through the inside of the Elbow piece, which has been removed for the purposes of this picture.

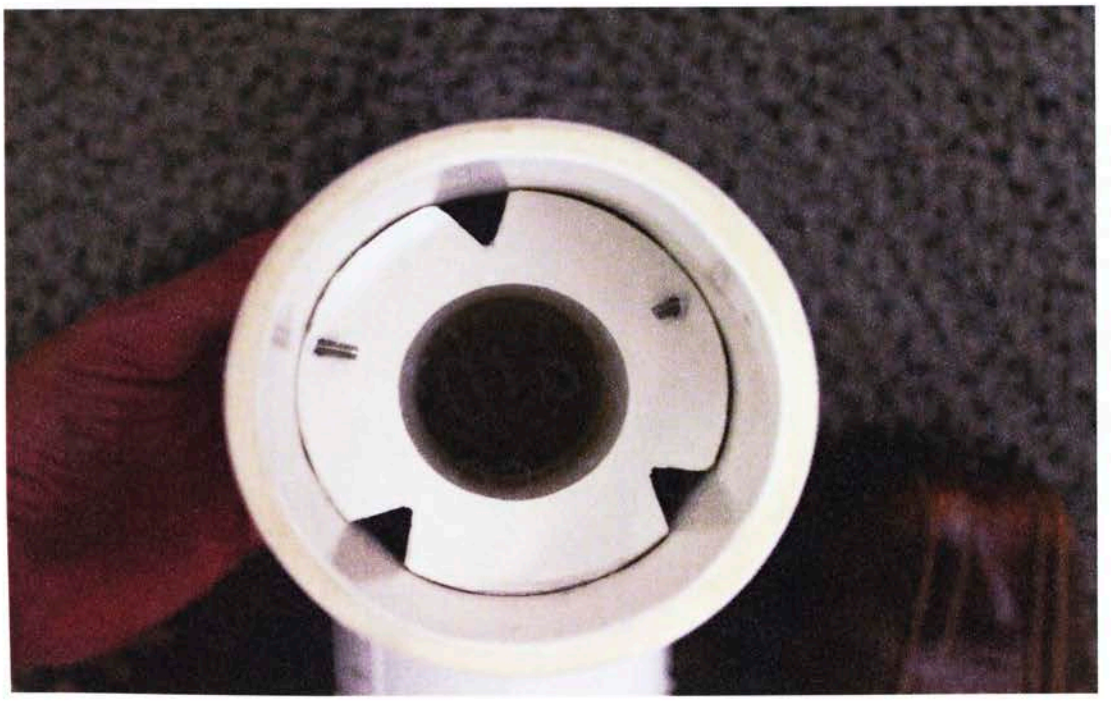

Figure 10: Image of the upper funnel with vent holes cut. The piece shown has only three triangular holes shown which was an earlier design; however the final design features 4 semi-circle shaped holes.

Figure 11: Charlotte Pipe PVC Pressure Schedule 40 Coupling. Used to join the intake section to the central housing section.

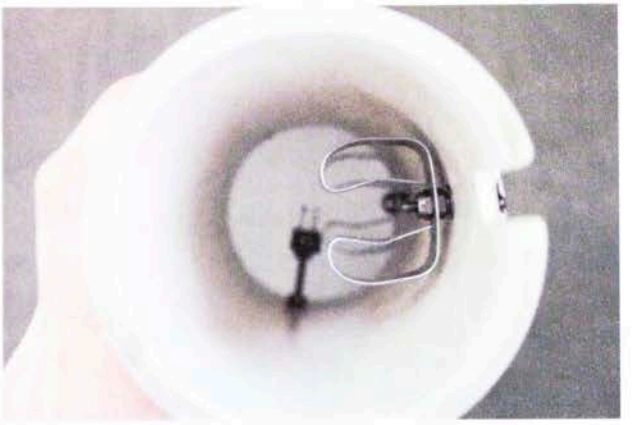

Figure 11: Central housing section showing mounting brackets for temperature and RH sensors. Sensors should be mounted so that the sensor heads stick slightly inside the flared funnel at the end of the intake section.

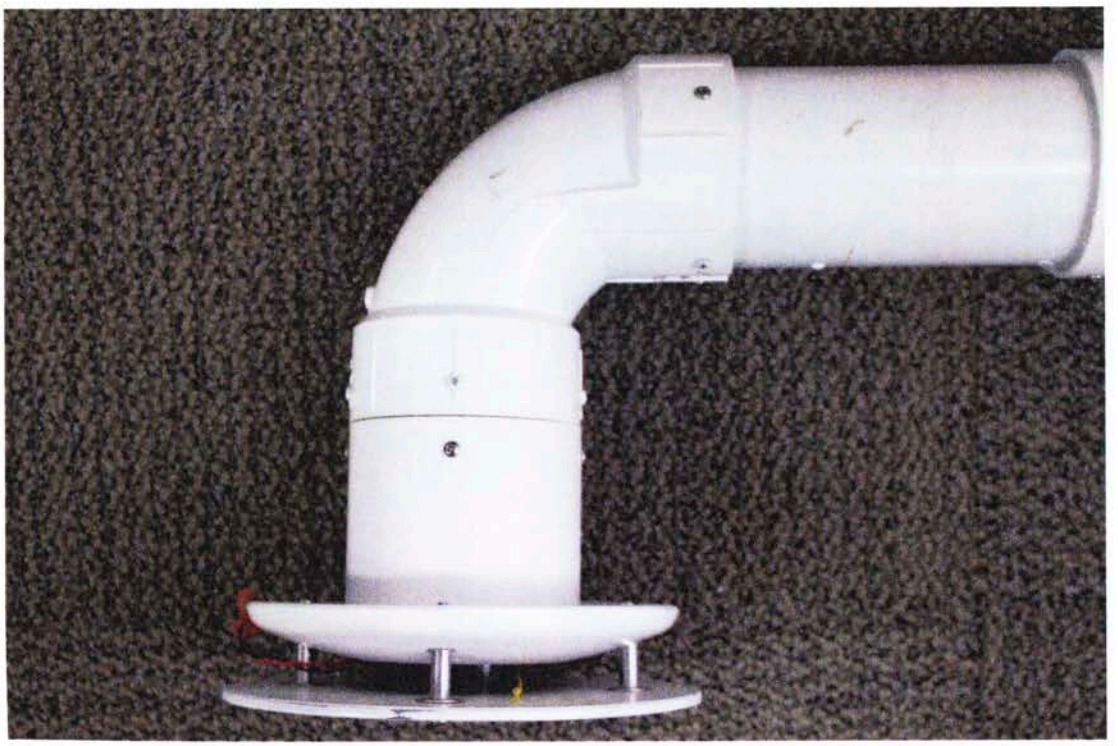

Figure 12: Image of the exhaust portion of the U-tube. This section features a curved plate above a flat plate to induce a Bernoulli Effect to help with flow acceleration. The wires protruding from below the curved plate are power wires for the DC fan located in the section.

Figure 14: Charlotte Pipe 4" PVC Pressure Schedule 40 Cap. The larger cylinder section was cut off, leaving only a large curved disk. Any size cap can be used to achieve a desired disk size and curve.

Appendix B: U-tube Construction

The following provides further detail on how to construct the various pieces of the U-tube. Additional images are provided in Appendix A to document the multitude of PVC pieces used to create the instrument. Note that the images shown are not necessarily the exact dimensions of the actual piece used, but are meant to demonstrate the type of piece used. In most cases, the piece used is modified to suit a specific function. The brand or exact dimensions of the product could be changed or modified to suit various needs or size requirements, but all pieces should be matched accordingly.

A. Intake

The intake (Appendix A, Figure 5) features two parallel plates, 8 inches (203.2 mm) in diameter, which are separated by 1 inch (25.4 mm) aluminum standoffs. Each of the two plates has an approximately 3.5 inch (88.9 mm) hole drilled through the center of the plate. The bottom plate has a small, hollow funnel epoxied directly to the plate, centered over the hole with the narrower end of the funnel pointing upwards.

This funnel was created by modifying a schedule 40 PVC pipe adapter that joins a 1 inch (25.4 mm) inner diameter pipe to a 3.5 inch (88.9 mm) diameter pipe (Appendix A, Figure 6). This adapter smoothly changes the size of the PVC from one diameter to the other and allows two sizes of pipes to be

connected. The larger, 3.5 inch (88.9 mm) section was cut off leaving only the flared funnel. The interior size of the funnel decreases from approximately 3.5 inches (88.9 mm) to 1 inch (25.4 mm) in diameter.

This two plate arrangement is attached to a 3.5 inch (88.9 mm) inner diameter 90° degree right angle piece (known as a 45° Elbow) (Appendix A, Figure 7), which leads to a 3.5 inch (88.9 mm) outer diameter piece at the top of the curve. The section is completed with a 1 inch (25.4 mm) , hand-made outer diameter, thin walled PVC piece (Appendix A, Figure 8) that curves through the inside of the larger curved piece, attaching to the bottom plate at the top of the funnel. Appendix A, Figure 9 shows how the inner tube is attached to funnel without the elbow piece.

This inner tube was created by hand so that it curved through the center of the elbow without coming in contact with any of the inside walls. This tube was created by taking a straight tube, 1 inch (25.4 mm) in diameter, and cutting small sections at opposing 7.5° angles. These individual small pieces were then rotated and epoxied together to achieve the angle and curve desired.

At the end of this inner tube, another funnel, created as before, is used to widen the inner tube out to the inside diameter of the straight 3.5 inch (88.9 mm) outer diameter piece. This funnel has 4 small (about 0.25 inch [6.35 mm] radius) semi-circle shaped sections cut into the outside edge of the funnel, giving it a 4-

leaf clover pattern (Appendix A, Figure 10). This is done to allow air movement between the inner tube and the inside of the outer tube to reduce solar radiation errors. This works by allowing the air between in inner tube and the outer tube to absorb (primarily thought conduction) the energy being reradiated from the outer PVC. This air absorbs this energy and correspondingly increases its temperature, but then passes the air through the system without interacting with the sensors.

B. Central Housing

The central housing is attached to the intake using a collar piece (Appendix A, Figure 11) designed to fit over the 3.5 inch (88.9 mm) outer diameter tubing. With the intake section fitting into one side of the collar, the other side has attached a straight piece of 3.5 inch (88.9 mm) outer diameter tubing that is approximately 8.125 inches (206.4 mm) long. This serves as the housing for the temperature and/or relative humidity sensors. The sensors can be mounted in any orientation, but should be near the center of the tube with the sensor heads sticking slightly into the funnel at the top of the inner tube as shown on the schematic in Fig 6. An image of the mounting brackets inside this section is shown in Appendix A, Figure 12. This is done to ensure the air flow being sensed originated solely from the inner tube and the underside of the bottom plate. It also places the sensors in the region of maximum airflow

through the tube. The end of the central portion features a small hole so that cables from the instruments can exit the housing. This is sealed with coaxial putty

C. Exhaust

The exhaust (Appendix A, Figure 13) is constructed similarly to the intake by using a 90° degree slow right angle piece. At the end of the 90° right angel piece, there is another collar similar to the collar adjoining the intake to the central housing, except that this collar is a slightly deeper version. This is done so that a small DC fan (30 ft^3/min or 0.014 m^3/s) can be placed inside the collar so that when the collar is attached to the right angle piece, the fan is held in place and pulls air through the intake of the shield and out the exhaust.

At the bottom of the collar piece, there is a small section of 3.5 inch (88.9 mm) inner diameter tubing that has a large curved plate attached to it. The curved plate is approximately 7.3 inches (185.4 mm) in diameter and has a 3.5 inch (88.9 mm) hole cut in the center of the plate. This plate was created by taking a large, 6 in (15.24 cm) PVC cap (Appendix A, Figure 14) and cutting off the cylinder section so that only a curved disk remained.

Similar to the intake section there is a flat plate, 8 inches (203.2 mm) in diameter, that is suspended ½" (12.7 mm) below the curved plate (measured near the center of the two plates) using aluminum standoffs.